

Fluidic Flexible Matrix Composite Wafers for Volume Management in Prosthetic Sockets

Melina Renee De La Hunt

Thesis submitted to the faculty of the Virginia Polytechnic Institute and State University in
partial fulfillment of the requirements for the degree of

Master of Science

In

Mechanical Engineering

Michael K. Philen, Chair

Robert L. West

Pablo A. Tarazaga

27 April 2015

Blacksburg, Virginia

Keywords: Smart prosthetic socket, Fluidic flexible matrix composite, Volume management

Fluidic Flexible Matrix Composite Wafers for Volume Management in Prosthetic Sockets

Melina Renee De La Hunt

ABSTRACT

Persons with transfemoral (above knee) and transtibial (below knee) prostheses experience changes in the volume of their residual limb during the course of the day. These changes in volume unavoidably lead to changes in quality of fit of the prosthesis, skin irritations, and soft tissue injuries. The associated pain and discomfort can become debilitating by reducing one's ability to perform daily activities. While significant advancements have been made in prostheses, the undesirable pain and discomfort that occurs due to the volume change is still a major challenge that needs to be solved. The overall goal of this research is to develop smart prosthetic sockets that can accommodate for volume fluctuations in the residual limb. In this research, fluidic flexible matrix composite wafers (f2mc) are integrated into the prosthetic socket for volume regulation. The f2mc's are flexible tubular elements embedded in a flexible matrix. These tubular elements are connected to a reservoir, and contain an internal fluid such as air or water. Fluid flow between the tubes and reservoir is controlled by valves. A linear finite element model has been created to better understand output response and stiffness of the f2mc wafers for different design variables. Results demonstrate that wind angle, latex thickness, and material selection can be used to tailor the wafers for different applications. Through experiments, f2mc's have been shown to achieve nearly 100% strain through the thickness when pressurized to about 482.6 kPa (70 psi). The displacement results shown through these tests show great promise in applications of socket integration to compensate for volume change.

ACKNOWLEDGEMENTS

Firstly, I would like to thank my advisor Dr. Michael Philen for his constant support and mentorship. His knowledge and experience was invaluable, and he taught me more in the three years I worked with him than many of the courses I took. I will always be grateful to him for all the time and energy he spent working with me through my projects.

I would also like to thank the undergraduates working on the project, Adrian Baily and Michael Heim, for their assistance in gathering experimental data, and a graduate student in the lab, Brady Doepke, for his help in setting up the code for the finite element model. Additionally, I would like to thank Dr. Robert West the time he spent working through issues in my finite element model with me, and for his course in finite element modeling that taught me a lot of useful skills that I have used in my research.

I would also like to thank my parents Mike and Theresa Mercier for their support throughout this process, and all the encouragement and advice they have given me throughout my academic career. They have always been there to listen when I needed to talk or vent about frustrations in my work. Last but not least, I would like to thank my husband Noah for his patience and emotional support throughout these past few years. Through all the highs and lows of my project, he has been there to celebrate with me in my successes and ease my stress.

TABLE OF CONTENTS

ABSTRACT	ii
ACKNOWLEDGEMENTS	iii
TABLE OF CONTENTS	iv
LIST OF TABLES	vi
LIST OF FIGURES	vii
NOMENCLATURE	ix
CHAPTER 1: INTRODUCTION	1
1.1 Motivation	1
1.2 Socket Stresses	2
1.3 Current Solutions.....	4
1.3.1 Fluid Filled Bladders.....	4
1.3.2 Vacuum-Assisted Suspension.....	5
1.4 F2mc wafers	7
1.5 Problem Statement, Objectives, and Approach.....	8
1.6 Thesis Overview	9
CHAPTER II: MODEL DEVELOPMENT AND VALIDATION	10
2.1 Composite Model Validation	10
2.2 F2mc Tube Validation.....	14
CHAPTER III: MODEL RESULTS.....	19
3.1 Free Displacement Model	19
3.1.1 Model Setup	19
3.1.2 Model Results	21
3.2 Model under Transverse Loading	26
3.2.1 Model Setup.....	26

3.2.2 Model Results	27
CHAPTER IV: EXPERIMENTAL DATA	33
4.1 F2mc Fabrication.....	33
4.2 Experimental Setup	34
4.3 Experimental Results.....	35
CHAPTER V: CONCLUSIONS AND FUTURE WORK.....	42
5.1 Conclusions	42
5.2 Future Work	43
REFERENCES	45
APPENDIX A: FIGURES AND TABLES	47
APPENDIX B: CODE	51
AB1: Code used for tube model validation.....	51
AB2: Codes used for multiple tube system parametric study	53
AB.2.1 MATLAB Code to create variable inputs for top loaded code in AB2.2.....	53
AB2.2 Python code to create free displacement model and extract displacement results	53
AB.2.3 MATLAB Code to create variable inputs for top loaded code in AB2.4.....	59
AB2.4 Python code to create top loaded model and extract displacement results	60

LIST OF TABLES

Table 1: Composite Layup Validation: Aluminum	13
Table 2: Composite Layup Validation Results: Graphite-Reinforced Composite.....	14
Table 3: Tube Validation with End Cap Force: Boundary Condition and Loads.....	16
Table 4: Boundary conditions for the two tube model	20
Table 5: Wafers used in Experimental Testing.....	34
Table 6: Material Properties for Composite Layup Validation	47
Table 7: Material Properties.....	47
Table 8: Tube Model Validation-Abaqus Results	47
Table 9: Equipment Specifications for Wafer Experimentation.....	50

LIST OF FIGURES

Figure 1: Common pressure points found in the socket of a transtibial amputee [14]. Zhang, M., et al., *Clinical investigation of the pressure and shear stress on the trans-tibial stump with a prosthesis*. Medical engineering & physics, 1998. 20(3): p. 188-198. Used under fair use, 2015 3

Figure 2: Patent drawing for a prosthetic socket containing inflatable bladders [16]. Love, M.G., *Prosthetic socket containing inflatable means*. 1995, Google Patents. Used under fair use, 2015. 5

Figure 3: Triton Harmony® elevated vacuum system [20]. Ottobock, *Below-knee prosthesis with: Triton Harmony*. 2013. Used under fair use, 2015. 6

Figure 4: Proposed prosthetic socket having embedded f2mc wafers located at critical areas for volume management 7

Figure 5: a) Contracting and extending f2mc actuators when pressurized, b) Coordinate system of the tubes, c) Example of an f2mc wafer 8

Figure 6: Square coupon used for material validation 11

Figure 7: Material squares used for composite layup validation [25] 12

Figure 8: Material Square Validation 13

Figure 9: Tube Model Validation 14

Figure 10: Tube Model Validation: Longitudinal Strain vs Wind Angle 17

Figure 11: Examples of f2mc wafer shapes 19

Figure 12: Two tube model 20

Figure 13: Boundary Conditions for two tube system model 21

Figure 14: Longitudinal strain vs wind angle validation 22

Figure 15: Wind Angle Validation at 70psi 23

Figure 16: Effect of different internal pressurizations as latex tubing thickness varies 24

Figure 17: Strain vs Internal Pressurization for Various Wind Angles 25

Figure 18: Strain vs Internal Pressurization for different values of Latex Thickness 26

Figure 19: Top loaded multiple tube system 27

Figure 20: Stress vs strain for passive stiffness with two different boundary conditions 28

Figure 21: Stress vs strain relationship for top loaded model one side constrained 29

Figure 22: Stress vs strain relationship for top loaded model two sides constrained 29

Figure 23: Stress vs strain for various carbon fiber layer thicknesses 30

Figure 24: Blocking stress vs internal pressurization for various boundary conditions	31
Figure 25: a) Small f2mc circular wafer before a fitting is applied, b) Small f2mc circular wafer after a fitting is applied, c) Larger elongated f2mc wafer.....	33
Figure 26: Experimental setup for compression testing of f2mc wafers	34
Figure 27: Stress vs strain relationship for experimental results of the large wafer.....	36
Figure 28: Different sizes of f2mc wafers tested.....	37
Figure 29: Stress vs strain relationship for experimental results of the small wafer	38
Figure 30: Free displacement vs internal pressure for Wafer 1 (large) and Wafer 2 (small)	39
Figure 31: Residual limb model for volume change.....	40
Figure 32: a) Identified areas of critical volume change from a patient at the VA Medical Center in Richmond, VA, b) elongated wafers integrated into a socket	41
Figure 33: Von Mises Stresses with the load of a 250 lb person at internal pressure of 100psi ..	48
Figure 34: Radial Stress with the load of a 250 lb person at an internal pressure of 100psi	48
Figure 35: Circumferential Stresses with the load of a 250 lb person at an internal pressure of 100psi.....	49
Figure 36: Longitudinal Stresses with the load of a 250 lb person at an internal pressure of 100psi	49

NOMENCLATURE

A	Area
d	Diameter
E	Young's modulus
G	Shear modulus
h	Height
P	Pressure
r	Radius
r_i	Inner radius
r_o	Outer radius
t	Thickness
u	Displacement
V	Voltage
V_f	Fiber volume fraction
V_i	Initial voltage
V_m	Matrix volume fraction
ε	Strain
γ	Shear strain
ν	Poisson's ratio
σ	Stress
σ_h, σ_L	Hoop Stress, Longitudinal Stress
Θ	Fiber angle

CHAPTER 1: INTRODUCTION

1.1 Motivation

It is estimated that 185,000 people undergo a limb amputation each year and more than 1.6 million people are living without a limb [1]. Approximately one million people in the United States are living with the loss of a lower-limb specifically, and about 90% of those amputations are the result of vascular disease [2].

Additionally, with Operation Iraqi Freedom, the amputation rate for United States troops has been twice as high as past conflicts [3]. One of the highest priorities for the Department of Veteran Affairs, is the care of veterans with major limb loss from combat [4]. In a survey conducted from veterans of the Vietnam and Operation Iraqi Freedom wars, 51% and 58% respectively reported prosthesis-related skin problems. Of those amputees from the Vietnam and Operation Iraqi Freedom wars, 71% of them suffered loss of limbs below the hip. Because of the recent conflicts in Iraq and Afghanistan, there is an increase in young amputees who wouldn't otherwise be disabled before a traumatic injury [2]. These patients have different needs from patients with vascular disease or other health problems.

For those who have lost a limb, a prosthesis may offer improved function during daily activities, a re-established appearance, and a better quality of life. However over the course of the day, the volume of the residual limb naturally changes during the day depending on activity level, environmental conditions, dietary habits, and prosthesis fit [5]. This volume change of the residual limb can cause discomfort in a prosthetic since the fit of the socket changes. The cause of volume change in the limb is an imbalance in the fluid volume moving from the arteries to the interstitial space and the fluid volume moving from the interstitial space into the lymphatics or veins [2]. This can cause pain and damage to the residual limb. It has been reported that the volume of the residual limb can change between +7% and -11% over the course of a day [6], and a volume change as small as 3% to 5% can cause difficulty and pain for the amputee [7]. About 90% of this volume loss occurs within the first 2 hours of activity [4]. Studies show that patients can experience around 0.10-0.12 mL of volumetric change per minute while standing and 0.20-0.30 mL per minute while resting after movement [8].

Transtibial amputees specifically, those who after amputation have a residual limb below the knee, have a muscle flap folded over the truncated shinbone [9]. The compression of this flap while wearing a prosthetic socket can cause high pressure and deep tissue injury. They unavoidably develop skin irritations and soft tissue injuries on and around their residual limb due to improper prosthetic fit. These injuries in the residual limb can lead to immobility and additional surgery [10]. About 80% of lower limb amputees have additional complications from peripheral vascular disease and/or diabetes as well [9]. Amputees with these problems have a reduced ability to detect pain which can increase the risk of deep tissue injury. By improving the fit of the prosthetic socket, it may be possible to reduce the loads on the residual limb and prevent deep tissue injury.

The single most critical aspect of any prosthesis is the interface between the limb and the prosthesis. Generally, liners are used to create a thin, comfortable, and compliant barrier between the amputee's skin and the prosthetic socket, and multiple liners can be worn depending on activity and comfort. These socket liners are usually connected to the inside of the socket with a mechanical lock or through a suction device to provide suspension for the limb. As the volume of the limb changes during the course of the day, the amputee must add or remove liners or sheaths to account for the volume change and to reduce the pain and discomfort [5, 11]. However, removing the prosthesis and changing liners during the day can be difficult and disruptive to the user's daily activities. Moreover, this approach does not have the ability to accommodate for volume changes over localized regions of the residual limb, which is typical among amputees [12]. While significant advancements have been made in prostheses, the undesirable pain and discomfort that occurs due to the volume change is still a major challenge that needs to be solved. The overall goal of this research is to create a socket interface that can improve this prosthetic socket fit by accommodating for volume change of the limb.

1.2 Socket Stresses

Based on current research in the field of prostheses, mechanics of the soft tissue and bone within the residual limb is very specialized to the individual, making it difficult to predict levels of shear stress and pain [9, 13]. There is evidence however that certain bony prominences are common pressure points for every transtibial amputee. In a study done by Zhang *et al.*, data from force transducers and a finite element analysis was used to characterize common pressure points

[14]. Figure 1 shows the locations within the socket that were found to bear the most pressure during standing and walking.

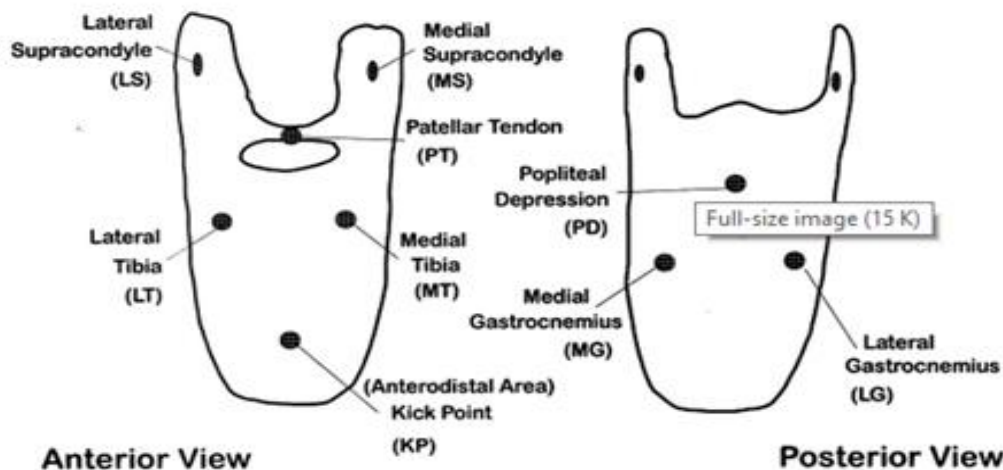


Figure 1: Common pressure points found in the socket of a transtibial amputee [14]. Zhang, M., et al., *Clinical investigation of the pressure and shear stress on the trans-tibial stump with a prosthesis*. Medical engineering & physics, 1998. 20(3): p. 188-198. Used under fair use, 2015

The three points on the posterior of the socket including the popliteal depression (back side of the knee), medial gastrocnemius (back side of lower leg), and lateral gastrocnemius (back side of lower leg) were found to be the points of highest pressure. Maximum peak pressure was 320 kPa from the popliteal region (back side of knee) during walking. Though the posterior (back side) points were those with the highest pressures during walking and standing, it wasn't the posterior portion of the limb where most patients were experiencing discomfort. The largest shear stress was 61 kPa in the medial tibial area on the anterior (front side) of the socket, and it was this high shear stress region that caused the amputee the most discomfort. Since there is a large expanse of soft tissue on the back of the lower leg, patients did not seem to experience as much discomfort due to the large distribution of force over that area. It appeared that common problem areas for most amputees were at the bony prominence areas such as the anterodistal (front and lower) area and the lateral (side) supracondyle of the tibia since the ends of the remaining bones are cut unnaturally and do not have very much soft tissue protection [14]. Since the volume, pressure, and spatial

location requirements vary among the patients, it is important that the socket can accommodate the volume change in the residual limb at the critical locations.

Another study by Faustini *et al.* used finite element methods to model the stresses at the interface of the patellar tendon on the prosthetic socket [15]. Four different socket designs were used to compare the stresses on the residual limb as a result of the socket: one baseline regular socket and three sockets with different compliant features incorporated. Using a computed tomography (CT) scan of a residual limb, a baseline finite element model of the system was created. A constant 800 N force was applied on the model to validate with literature. Quasi-static loading was used to simulate activity. With the baseline constant load of 800 N, the socket produced a maximum pressure of 250 kPa at the patellar tendon. For all four sockets, the maximum pressure on the fibula head was found at 75% of the stance phase. A regular socket had a maximum pressure of about 172 kPa, and the thin-wall compliant socket had the largest pressure of all the compliant sockets with a maximum pressure of 135 kPa. This shows that adding compliant features into the socket will effectively drop the maximum pressure on the fibula head.

1.3 Current Solutions

1.3.1 Fluid Filled Bladders

As seen below in Figure 2, one solution currently on the market is to use fluid filled rubber bladders to fill in areas where volume reduction has occurred [16]. These bladders are placed into a double wall socket in areas where volume shrinkage is thought to occur.

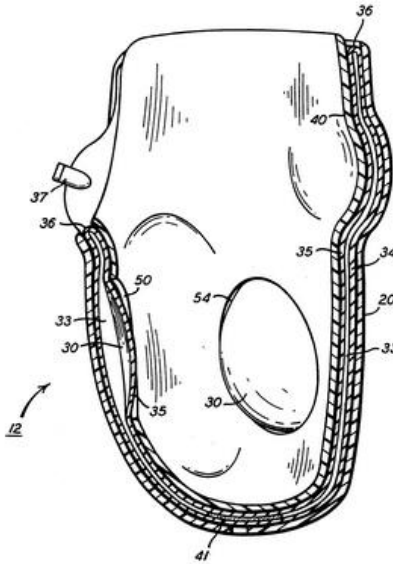


Figure 2: Patent drawing for a prosthetic socket containing inflatable bladders [16]. Love, M.G., *Prosthetic socket containing inflatable means*. 1995, Google Patents. Used under fair use, 2015.

One issue with air-filled inserts is that they cannot accommodate a large range of volume change [2]. Using fluid provides a larger dynamic range for volume change than water, and can reduce the shear to pressure ratio. However, they also show an increase in total interface stress. This additional pressure on the limb can cause an additional increase in volume loss [6]. These bladders can cause greater damage than a socket with no bladder because of over inflation causing damage to the limb. A common problem is that patients who experience a loss of sensitivity in the residual limb, such as diabetic patients, or patients that have difficulties with self-adjustments tend to over-inflate the system, thereby causing irreversible damage to the limb. Furthermore, air bladders do not provide the support to prevent movement between limb and socket in rotation and pistoning, and the coefficient of friction between the stump-liner and liner-socket must be high to limit movement at these interfaces [17, 18].

1.3.2 Vacuum-Assisted Suspension

Vacuum-assisted suspension method of volume control was introduced about 15 years ago [19], which uses a vacuum of about -80 kPa to suck the liner tightly against the socket [6]. Vacuum-assisted suspension systems create this vacuum to decrease the interstitial fluid pressure within the limb during gait [2]. One of the most commonly used vacuum-assisted suspension systems used is the Harmony® Vacuum-Assist System (Figure 3).



Figure 3: Triton Harmony® elevated vacuum system [20]. Ottobock, *Below-knee prosthesis with: Triton Harmony*. 2013. Used under fair use, 2015.

Ideally, the decrease in fluid pressure provided by the vacuum would restore the balance of fluid movement and eliminate volume change. However, this system has been shown to maintain or increase the volume of the residual limb when worn [19]. This increase in volume can cause an increase in socket pressures which cause blood flow restriction and buildup of starved cells causing increased cellular waste development in the tissues. The magnitude of this increase in volume between high and low vacuum settings varied across different types of vacuum pumps. Electronic vacuum pumps showed a volume increase of about 0.6-1.9%, while the Harmony® pump had a much lower percentage from high and low vacuum settings of 0-0.7% volume change. Additionally, many doctors will not use these systems on patients with comorbidities because they are afraid that the vacuum would worsen the tissue damage [2].

Sample size has also been discussed as a problem in these studies. The viability and success of vacuum pumps have been reported for very small sample size studies. With so much variability in the field of prosthetic design, it is impossible to say how all patients will react to this system when looking at a small sample. Additionally, without being able to use this system on patients' with co-morbidities, the number of patients able to benefit from this solution shrinks.

1.4 F2mc wafers

The system proposed here as a solution to increase prosthesis comfort through volume management in the socket is the f2mc wafer. F2mc wafers consist of fluidic flexible matrix composite tubes integrated into a polymer matrix to form a wafer that can change shape and volume. These wafers can be inserted in the wall of the socket at critical regions as illustrated in Figure 4.



Figure 4: Proposed prosthetic socket having embedded f2mc wafers located at critical areas for volume management

Key to the f2mc wafers are the fluidic flexible matrix composite tubes that were developed by Philen *et al.* [21-23] and consist of a latex tube surrounded by a matrix of stiff reinforcing fibers, such as carbon fiber. When pressurized with a fluid, the actuators can either contract or extend axially depending on fiber orientation (Figure 5). For example, for angles less than 54.7° , the actuator shortens in length while expanding radially (i.e. contracting actuator) and the actuator extends in length for angles greater than 54.7° (i.e. extending actuator) [24]. Furthermore, these actuators can achieve a large change in stiffness when using a high bulk modulus fluid and simple valve control [23]. When the valve is open, the tubes are soft in the axial direction. However, when the valve is closed, the high bulk modulus fluid resists any volume change from the applied force, resulting in a large effective stiffness. Stiffness changes as large as 52 times has been measured in the laboratory [23].

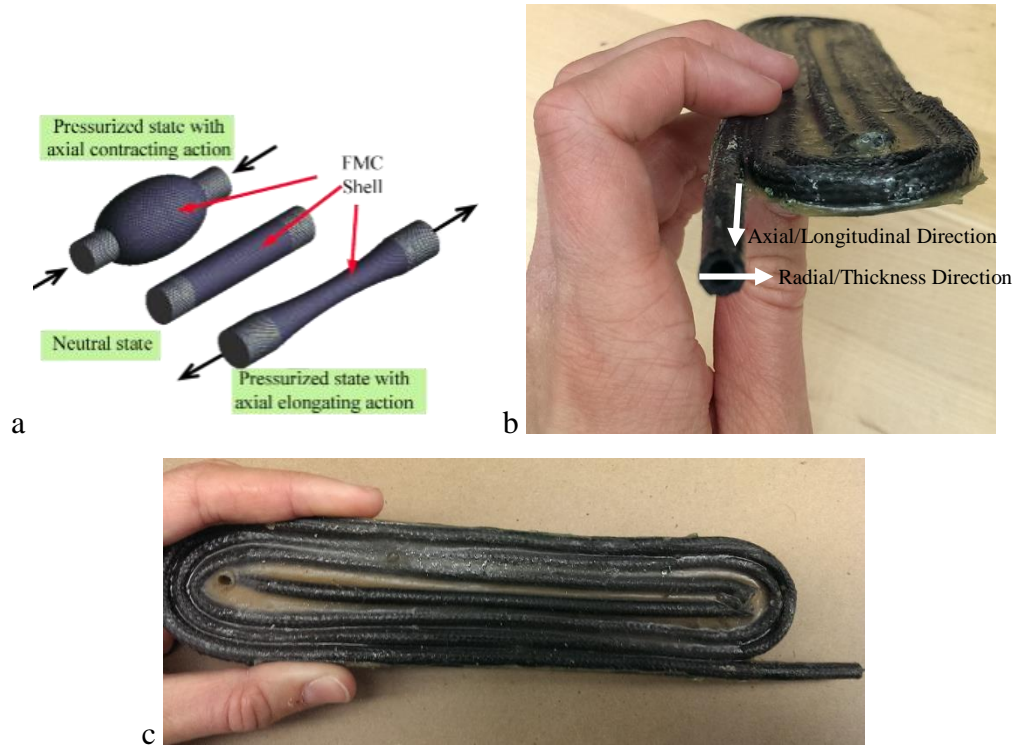


Figure 5: a) Contracting and extending f2mc actuators when pressurized, b) Coordinate system of the tubes, c) Example of an f2mc wafer

Because sockets are already made custom for each patient, these f2mc wafers would be easily incorporated into the wall of the socket in specific areas of volume change. As needed throughout the day, the patient would activate any areas within the socket that was decreasing in volume to fill in that volume loss and provide support. This could help maintain a high level of comfort, protect the residual limb against high pressure points, and increase the time that the prosthesis can be worn. Unlike bladder systems, the change is uniform across the thickness and the f2mc wafers can sustain large shear loads with minor deformation.

1.5 Problem Statement, Objectives, and Approach

As discussed, prosthesis fit is a major problem that has not been fully solved by currently available solutions. A new proposed solution is to use f2mc wafers integrated into the socket. However, while great research has been performed for f2mc actuators in the axial direction, no research has been performed for the tubes and wafers in compression through the thickness. The wind angle is important for tailoring the response of the actuator in the axial direction, but it not known how the wind angle will affect the response of the wafer in the thickness direction. Therefore the objectives

of this research are to investigate the effects of wind angle, latex thickness, composite tube thickness, internal pressurization, and top loading force on the strain of the system in the thickness direction. Additionally, the characteristic stress vs strain curve of this system in compression is of great interest for design.

To achieve the objectives of this research, our approach is to develop a simplified model of the f2mc wafer using finite element analysis and investigate the performance of the wafer for different operating and loading conditions. Experimental data from physical wafers under a compression plate will also be used to explore the behavior of this system, and compare results with the finite element model.

1.6 Thesis Overview

The overall structure of this thesis is as follows. Chapter 1 presents an overview of the need for improvements to the comfort of prostheses. It also discusses current state of the art solutions to this problem, and where improvements can be made to these current methods. Next, the proposed solution of f2mc wafers is introduced as a system that has great tailorability, stiffness support, and uniform displacement. Finally, the approach to model these materials and explore this application are discussed. Chapter 2 details the derivation of the composite model used to create a finite element model of the f2mc tube system. It also discusses the various simplified models created to validate the setup of the final model. These validation results are compared to theoretical calculations and used for the final model created in Chapter 3.

Chapter 3 introduces free displacement and top loaded two tube models created based on the validations in Chapter 2. It discusses the results for stress and strain in the system for different variations of several parameters including: carbon fiber wind angle, latex tube thickness, carbon fiber layer thickness, internal pressurization, and top loading.

Chapter 4 explores the experimental results obtained from small and large physical f2mc wafers. The amount of achievable volume change is compared to the expected amount seen in a prosthesis. Finally, the results for stress and strain are then compared with those in the finite element model, and hypotheses are made about the discrepancy between the two.

Chapter 5 includes conclusions about the results found through Chapter 3 and 4, as well as future work for this research.

CHAPTER II: MODEL DEVELOPMENT AND VALIDATION

Studying the response of f2mc wafers and tubes in compression through the thickness is a difficult problem and no simple closed form solutions exist. Therefore, finite element analysis is used for modeling the actuator and analyzing the response.

To create an accurate finite element model, it is important to examine the makeup of an f2mc wafer. F2mc wafers have three basic components: a latex tube, a flexible sheath over the latex tube with stiff reinforcing fibers (i.e carbon fiber), and a supporting rubber matrix molded over the entire system. The flexible sheath component of the f2mc wafers rely on stiff reinforcing fibers embedded in a soft elastomeric resin forming the wall of the tube. As result, the laminate is highly anisotropic with an E_1/E_2 ratio greater than 1×10^4 and the response of the actuator is highly dependent on the fiber wind angle. Therefore it is important to accurately model the fiber reinforced composite forming the wall of the tube.

To do this, several validations are completed to check the accuracy of modeling this difficult composite system. The first step in developing an accurate model is to validate the composite material creation. To do this, a square coupon model with a closed form solution is used (2.1 Composite Model Validation). In this model, various fiber angles are used to compare the finite element model resulting strains to the calculated values from the hand solution. After validation of this simple model, a more complex tube model is formed (2.2 F2mc Tube Validation). Moving into a cylindrical layup of the composite, a simple hoop and longitudinal stress calculation is made to validate the stresses on the system, and the strain curve of a composite with various fiber wind angles is used to validate further.

Using the validated composite material layup, the final multi-tube finite element model can be created.

2.1 Composite Model Validation

One important step in the process of creating a model for this f2mc system is to validate the model against known solutions. Using a square material coupon with a known hand solution, an Abaqus model can be created to validate the composite layup with fibers of different angles (Figure 6).

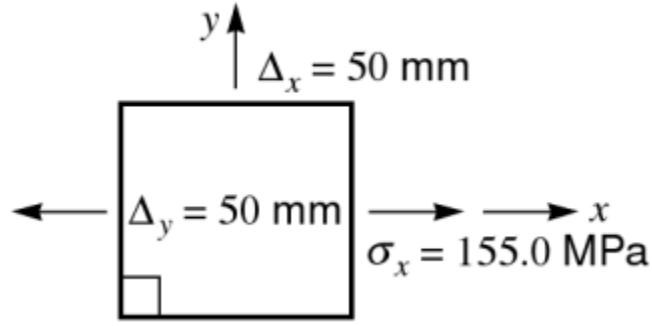


Figure 6: Square coupon used for material validation

For an isotropic material such as aluminum, the following relationships are used in calculating strain given a certain normal tensile stress σ_x :

$$\varepsilon_x = \frac{1}{E} \sigma_x$$

$$\varepsilon_y = -\frac{\nu}{E} \sigma_x$$

$$\gamma_{xy} = 0 \times \sigma_x$$

For a composite model with fibers oriented in a certain direction, the relationship for strains in this model becomes:

$$\varepsilon_x = \bar{S}_{11} \sigma_x$$

$$\varepsilon_y = \bar{S}_{12} \sigma_x$$

$$\gamma_{xy} = 0 \times \sigma_x$$

where \bar{S}_{11} and \bar{S}_{12} depend on the angle θ of the fibers.

$$\bar{S}_{11} = \frac{1}{E_1} m^4 + \left(-\frac{2\nu_{12}}{E_1} + \frac{1}{G_{12}} \right) n^2 m^2 + \frac{1}{E_2} n^4$$

$$\bar{S}_{12} = \left(\frac{1}{E_1} + \frac{1}{E_2} - \frac{1}{G_{12}} \right) n^2 m^2 + \frac{-\nu_{12}}{E_1} (n^4 + m^4)$$

where $m = \cos\theta$ and $n = \sin\theta$

As a benchmark hand solution, the composite material square example provided by Hyer’s textbook “*Stress Analysis of Fiber-Reinforced Composite Materials*” is used. First, an aluminum square is loaded as shown in Figure 7(a), then a graphite composite at different angles is built as shown in Figure 7(c,e). The material properties for these models can be found in the Appendix in Table 6. The materials chosen (aluminum and graphite composite) are used so that an accurate comparison to the hand calculation provided by Hyer can be achieved in the Abaqus model.

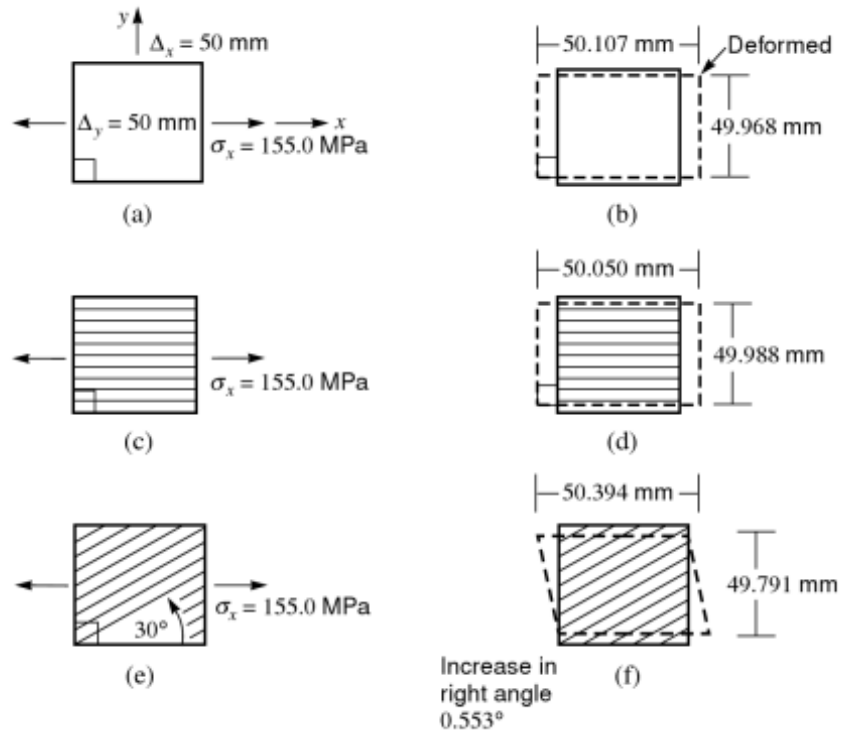


Figure 7: Material squares used for composite layup validation [25]

The Abaqus model for comparison uses 3D Brick elements (C3D8R elements), and has a fixed boundary condition at the bottom surface and a normal stress of 155 MPa on the sides (Figure 8).

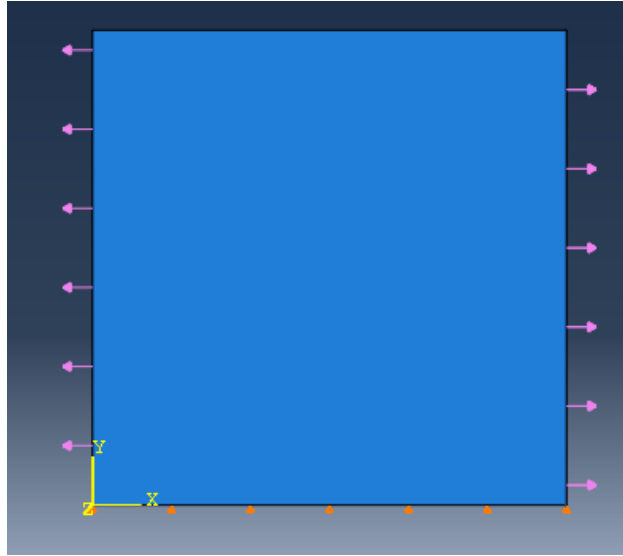


Figure 8: Material Square Validation

The resulting deflections shown in Figure 7 (b,d,f) are compared with the Abaqus model to verify an accurate composite layup method. The strains in each model are also used to compare the Abaqus solution to the hand calculation given by Hyer (Table 1 and Table 2).

Table 1: Composite Layup Validation: Aluminum

Aluminum			
	Abaqus	Hyer Calculation	% diff
ϵ_x	2.14E-03	2.14E-03	0.047%
ϵ_y	-6.42E-04	-6.42E-04	0.047%
γ_{xy}	0	0	0.000%
U1 (mm)	50.107	50.107	0.000%
U2 (mm)	49.9679	49.968	0.000%

Table 2: Composite Layup Validation Results: Graphite-Reinforced Composite

Graphite Composite						
	30 degrees			-30 degrees		
	Abaqus	Hyer Calculation	difference	Abaqus	Hyer Calculation	difference
ϵ_x	7.88E-03	7.88E-03	0.06%	7.88E-03	7.88E-03	0.06%
ϵ_y	-4.17E-03	-4.17E-03	0.02%	-4.17E-03	-4.17E-03	0.02%
γ_{xy}	-9.64E-03	-9.64E-03	0.03%	9.64E-03	9.64E-03	0.03%
U1 (mm)	50.876	50.394	0.96%	50.876	50.394	0.96%
U2 (mm)	49.7915	49.791	0.00%	49.7915	49.791	0.00%

With no more than 1% difference between the Abaqus model and the hand calculation, the composite layup model in Abaqus is verified. With the square verified, the same material layup used in the square will be used in the shape of a cylinder to form the carbon fiber tube that more accurately represents the final desired system.

2.2 F2mc Tube Validation

Moving to a cylindrical composite, carbon fiber is used to validate the final desired model of the flexible sheath layer of the f2mc wafer. The tube is validated for various wind angles before incorporating it into the entire f2mc wafer. To do this, a tube model with a 2-ply carbon fiber composite layup and 3D brick elements (8000 C3D8R elements) is created in Abaqus (Figure 9). A 2-ply layup through the thickness direction is used because the physical carbon fiber sheath in the wafer is a braided sleeve which means it has two lines of fibers, one at $+\theta$ and one at $-\theta$ (where θ is the wind angle with respect to the horizontal axis).

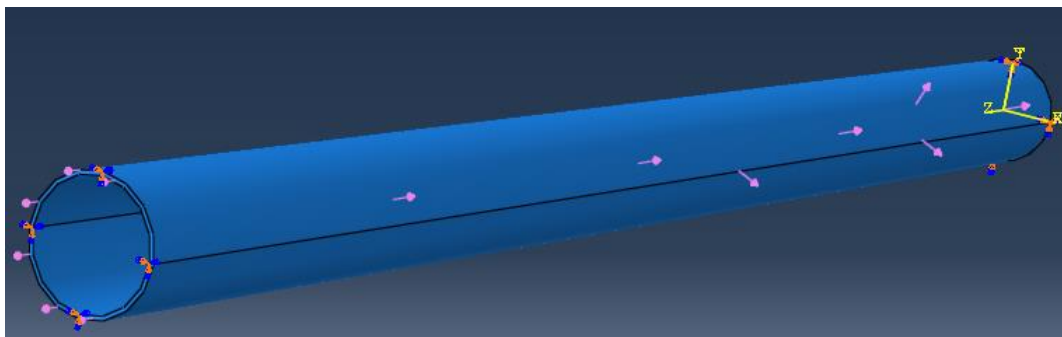


Figure 9: Tube Model Validation

To find the material properties of the carbon fiber composite layup, a fiber/matrix composite approach is used. The composite is modeled as a combination of carbon fiber fibers with a Vytaflex® 20 rubber matrix. The fraction of fibers in the volume (V_f) is assumed to be 50% (0.5) [26]. The effective Young's modulus, Poisson ratio, and shear modulus are found using the following equations:

$$E_{11} = fE_{1f} + (1 - f)E_{1m}$$

$$f = \frac{V_f}{V_f + V_m}$$

where E_{1f} and E_{1m} stand for the Young's modulus of the carbon fiber and rubber respectively, V_m and V_f are the volume fraction of the matrix and fiber respectively, and E_{11} is the overall effective Young's modulus along the fiber direction. The effective Young's modulus perpendicular to the fiber direction (E_{22}) is calculated:

$$E_{22} = E_{33} = \frac{E_{2m}E_{2f}}{E_{2m}V_m + E_{2f}E_{2m}V_f}$$

Because the material is orthotropic, $E_{22}=E_{33}$. To find the effective Poisson ratios (ν_{12} , ν_{13} , and ν_{23}) the following equations are used:

$$\nu_{12} = \nu_{13} = V_f\nu_{12f} + V_m\nu_m$$

$$\nu_{23} = V_f\nu_{23f} + V_m\nu_m$$

where ν_{12f} (or ν_{23f} , ν_{13}) and ν_m are the Poisson ratios of the fiber and matrix respectively. The final material property of interest is the shear modulus. The values for G_{12} , G_{13} , and G_{23} are calculated using the following equations:

$$G_{12} = G_{13} = \frac{G_m * G_{12f}}{G_mV_f + G_{12f}V_m}$$

$$G_{23} = \frac{E_{22}}{2 * (1 + \nu_{23})}$$

The material properties used for the matrix (Vytaflex® 20) and fiber (carbon fiber) can be found in Table 7 in the Appendix.

To load the system, an internal pressurization is applied in the tube, and a longitudinal force is applied at one end of the tube to simulate the effects of an end cap. The value of the end cap force is calculated and converted into a surface pressure using the following equations:

$$F_{end} = PA_{end}$$

where $A_{end} = \pi r_i^2$ and P = Internal pressure

$$P_{end} = \frac{F_{end}}{A_{cs}}$$

where $A_{cs} = \pi r_o^2 - \pi r_i^2$ = Area of the cross section

The boundary condition applied, fixes the back end of the tube and allows free movement at the other end (Table 3).

Table 3: Tube Validation with End Cap Force: Boundary Condition and Loads

Boundary Condition	
<i>Back</i>	Fixed
Loads	
<i>Internal Pressure (P)</i>	0.1 MPa
<i>Front End Cap Pressure (P_{end})</i>	0.738294 MPa

The displacement along the longitudinal axis is measured and compared to a simple axisymmetric thin-walled cylindrical shell model having uniform displacement along its length. As can be seen below in Figure 10, the composite tube Abaqus model matches closely with the behavior from the theoretical solution. One important point to note is the “locking angle” at which

the tube switches from negative to positive longitudinal strain, and positive to negative radial strain. This angle occurs at about 55 degrees in both the model and theoretical solution. At this angle, the actuator will no longer deform with increasing pressure. The code used to generate the theoretical solution can be found in Appendix B, and the results plotted from the Abaqus model can be found in Table 8.

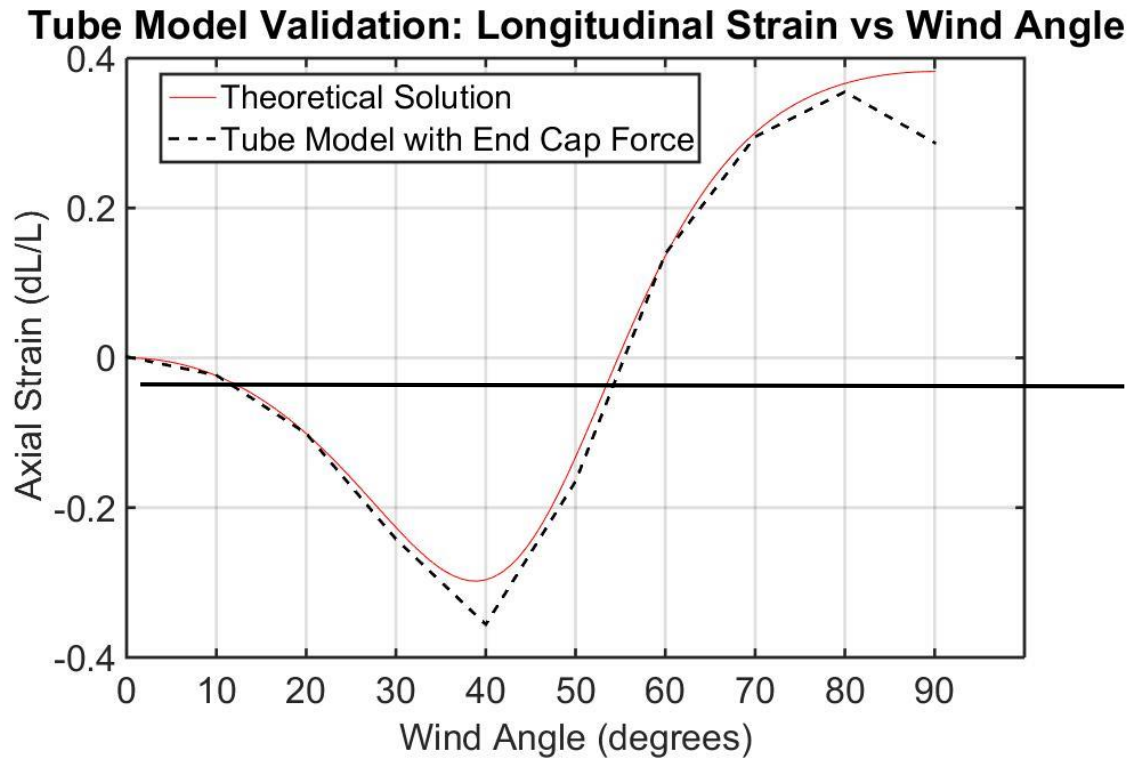


Figure 10: Tube Model Validation: Longitudinal Strain vs Wind Angle

The expected hoop (σ_h) and longitudinal (σ_L) stresses were also used to validate this model. The expected values for these stresses can be calculated using thin wall pressure vessel equations:

$$\sigma_h = \frac{Pd}{2t}$$

$$\sigma_L = \frac{1}{2}\sigma_h$$

In this model, $d=6.5$ mm, $t=0.2$ mm, and $P=0.1$ MPa, so the expected hoop stress was 1.625 MPa and the expected longitudinal stress was 0.8125 MPa. To compare these values to the finite element model, the average of the stresses in each ply of the two ply model of carbon fiber was used. The stresses at different wind angles were examined, and the average of the hoop and longitudinal stresses for 10-90 degrees was calculated to be 1.507 MPa and 0.728 MPa respectively. With only 9% and 7% difference from the hand calculation in the hoop stress and longitudinal stress respectively, the stress in the tube model agreed well with theoretical values for a cylindrical pressure vessel. Now, a multiple tube system with all components of an f2mc wafer can be created to compare to experimental results of the physical system.

CHAPTER III: MODEL RESULTS

The entire f2mc wafer is a complicated system consisting of an array of multiple tubes side by side in a variety of desired configurations (Figure 11). These different configurations are essential because every amputee will have different needs for where the wafers are placed. The location and shape of a bony prominence on the residual limb has a large influence on where the wafers would be placed to prevent loss of volume and discomfort. This also means that the shape of the actuator could be anything from a large L-shaped spiral to a small tight circle, or anything in between.



Figure 11: Examples of f2mc wafer shapes

As a first step for modeling a wafer, we are considering two tubes next to each other in a straight line to simplify the model. This two tube model is useful in exploring the interaction that occurs between each tube in the wafer.

3.1 Free Displacement Model

3.1.1 Model Setup

To create this two tube simplified model of the f2mc wafer, two single composite tubes (validated in Section 2.2) with a latex tube inside are placed next to each other with a surrounding rubber matrix of VytaFlex[®] 20 (Figure 12). The front end of the tubes has a physical end cap, and the back end is open with symmetric boundary conditions ($U_3=0$). The same carbon fiber composite tube and end caps made of aluminum are used here as before in the single tube validation. The surrounding rubber matrix is VytaFlex[®] 20 and the tube inside the carbon fiber is made of latex (material properties in the Appendix, Table 7).

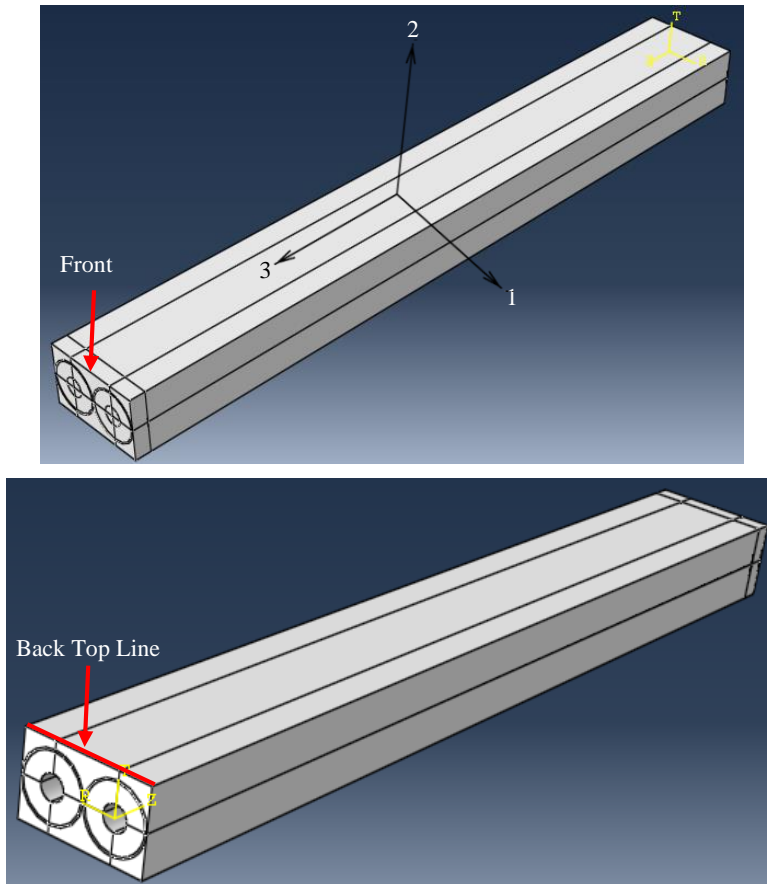


Figure 12: Two tube model

The aluminum end cap and carbon fiber are made up of 3D brick elements (C3D8R). The latex tube and surrounding rubber are hybrid elements (C3D8RH) because their Poisson ratios are close to 0.5. The surfaces on the top, front and one side were free, and all other boundary conditions can be found in Table 4 and Figure 13.

Table 4: Boundary conditions for the two tube model

Bottom	$U_2=0$
One Side	$U_1=0$
Back	$U_3=0$

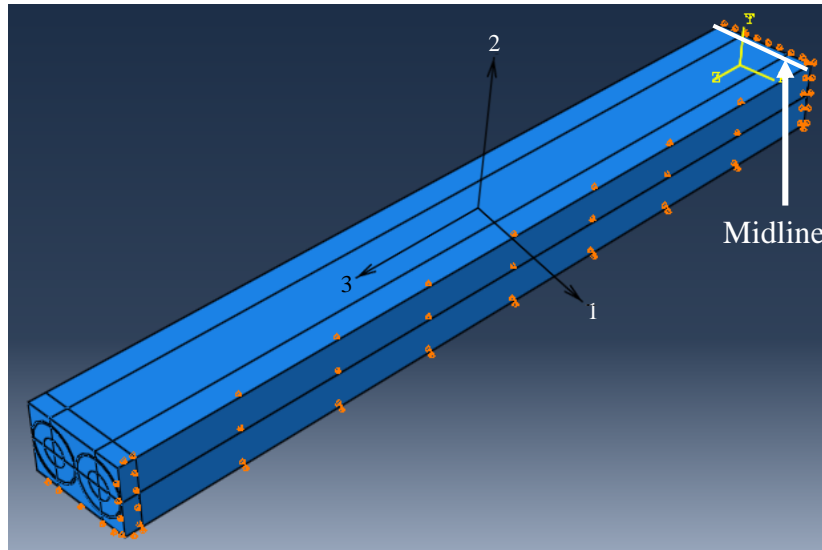


Figure 13: Boundary Conditions for two tube system model

The only loading in the system for the free displacement case is the internal pressurization inside the tubes. The values tested for pressure in this study ranged from 6.8948 - 48.263 kPa (10-70 psi). The effect of the wind angle of the carbon fiber was also tested for a variety of values ranging from 0-90 degrees. The thickness of the latex tubes was varied through different values ranging from about 0.55mm to 1.2mm. To evaluate all combinations of these variables (internal pressure, wind angle, tube thickness), a parametric study was created (code included in Appendix B). All tests were run using the Linear Solver in Abaqus. The results for displacement reported were found at the top line of the “back” of the model shown in Figure 12. This line represents the midline of the full system.

3.1.2 Model Results

As before with the single tube model, the longitudinal and radial strains of the system are of interest because of their great dependency on wind angle of the carbon fiber sheath. It is expected that at a wind angle of about 55 degrees, the longitudinal strain would move from negative to positive. A single node at the end of the tube was used as a reference node to track longitudinal displacement of the system through different wind angles (Figure 14). These results show a locking angle of about 55 degrees which agrees with the results found when a single carbon fiber tube was validated in Chapter 2.

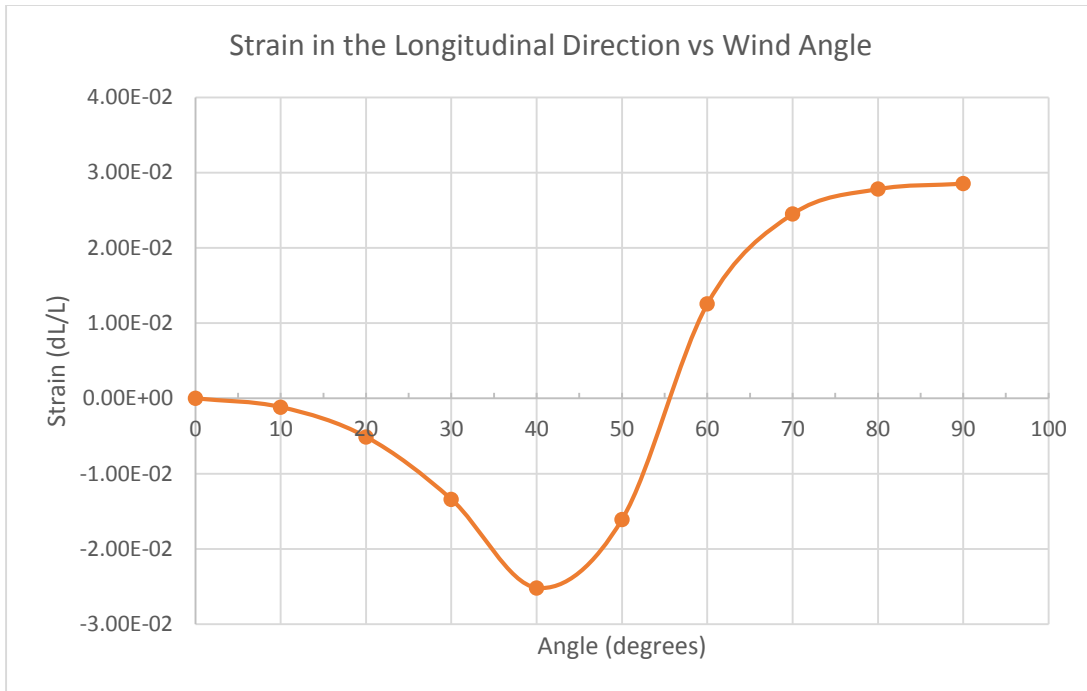


Figure 14: Longitudinal strain vs wind angle validation

Since the objective is to provide changes in thickness to accommodate volume change in the prosthetic socket, the variable of interest is the displacement through the thickness of the f2mc system with respect to the thickness (dt/t). It is expected that at the same locking angle of about 55 degrees, the strain through the thickness of the system would move from positive to negative as the tubes switched from contracting to expanding longitudinally. To simultaneously test the effect of the thickness of the latex tubing on the system, for a uniform internal pressurization of 206.84 kPa (30 psi), three different thickness values for the latex were tested (0.85mm, 1.05mm, and 1.25mm) through a range of wind angles from 0-90 degrees by increments of 10 degrees (Figure 15). As expected, for each different thickness value, the strain in the thickness direction at the midline shown in Figure 13 crossed from positive to negative at about 57 degrees. It can also be seen that the relationship between wind angle and strain is a highly non-linear relationship. Additionally, these results show that as the latex tube gets thinner, the magnitude of the strain in the thickness direction gets larger. With this knowledge, the materials used in the system can be optimized for greatest strain by reducing the thickness of the latex tubing. However, thinner tubing will also be more likely to fail, so a trade study would be necessary to weigh both variables to pick an ideal thickness.

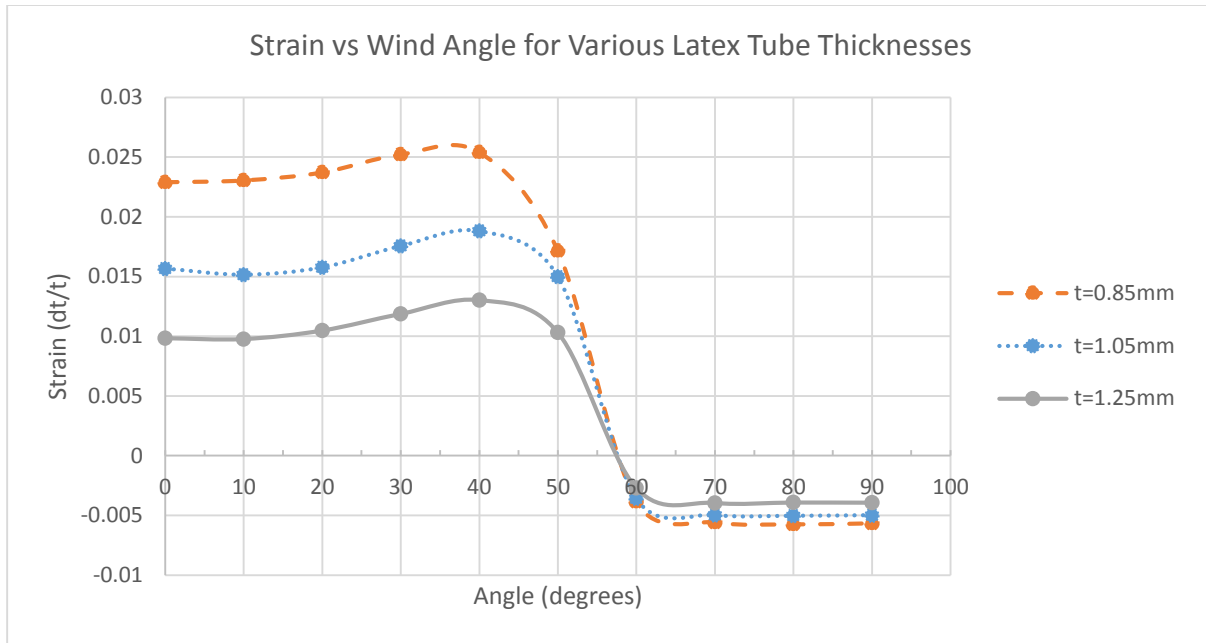


Figure 15: Wind Angle Validation at 70psi

From this graph, picking out the optimal peak of about 40 degrees wind angle, the relationship between different values of internal pressurization were explored. For three different values of internal pressurization 482.6, 344.7, and 206.8 kPa (30, 50, 70 psi), the relationship between latex thickness and strain was determined (Figure 16). The relationship found through these results shows that at higher internal pressurization, in a free displacement model, there is an increase in the strain through the thickness direction. It also expresses a non-linear relationship between latex thickness and strain.

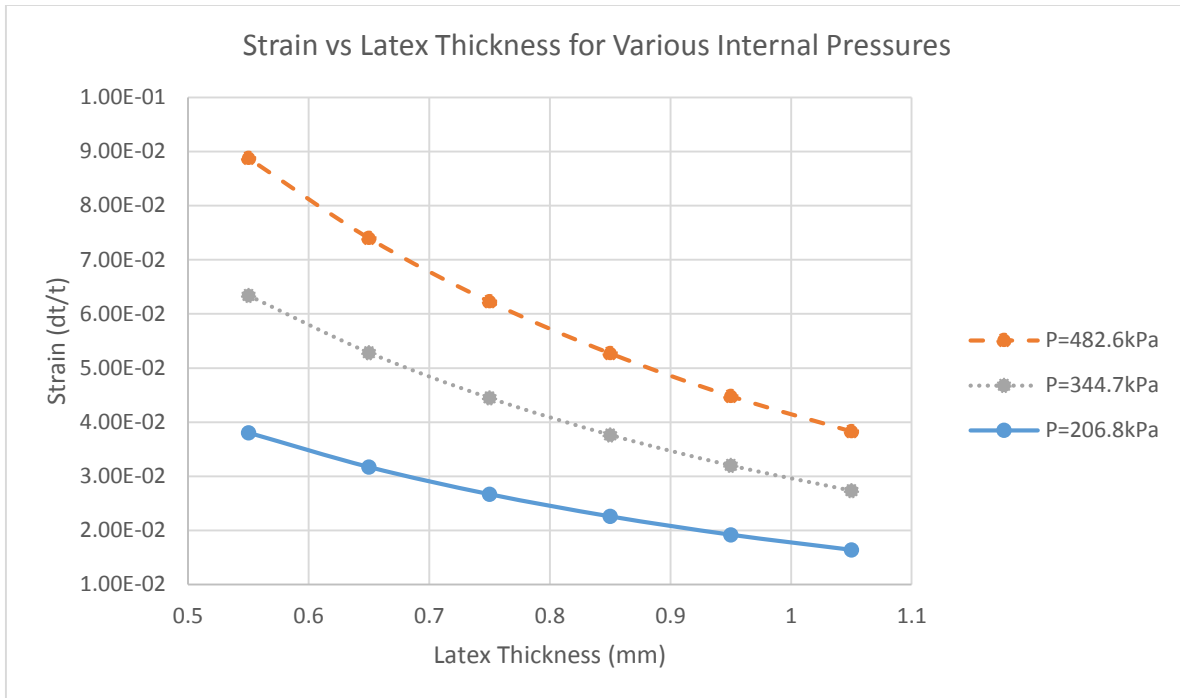


Figure 16: Effect of different internal pressurizations as latex tubing thickness varies

The relationship between internal pressurization and thickness strain is investigated for various wind angles. To capture this relationship, the internal pressure was varied from 0.06896 to 0.758 MPa (10 to 110psi), and the maximum value of displacement (either maximum positive or maximum negative) along the midline (see Figure 13) was recorded and converted into strain (Figure 17). This relationship shows a linear increase in strain as internal pressurization magnitude increases.

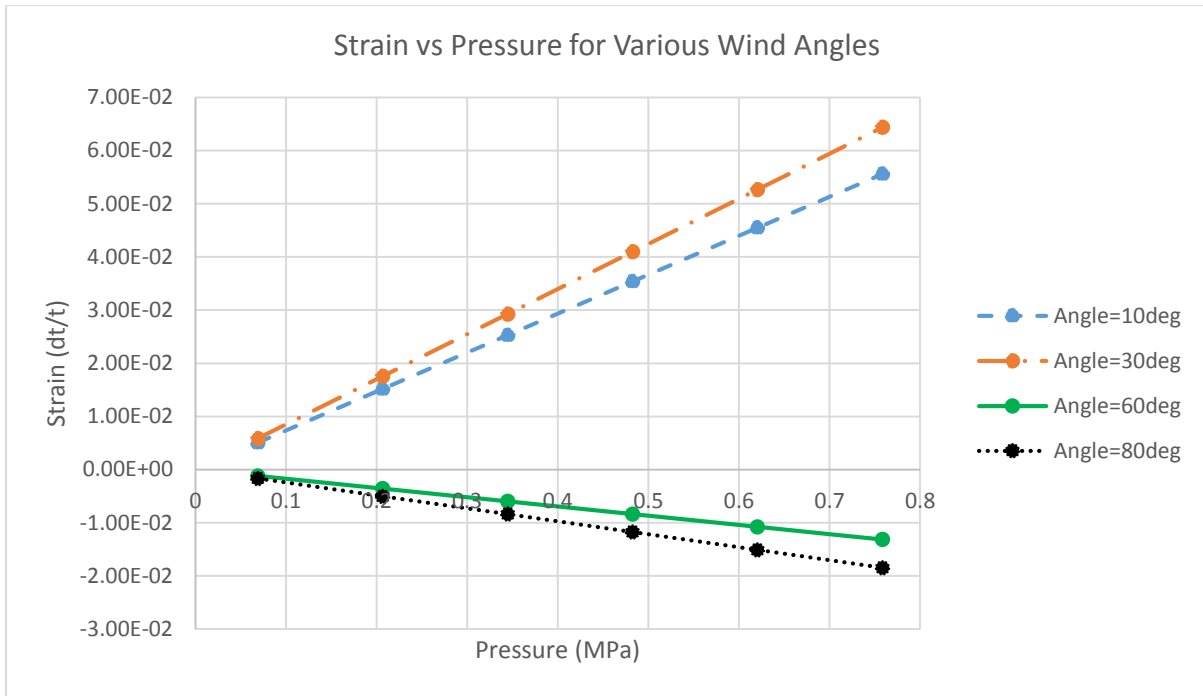


Figure 17: Strain vs Internal Pressurization for Various Wind Angles

Next, the relationship between internal pressurization and thickness strain was investigated for various thicknesses instead of wind angles. For this relationship, a wind angle of 30 degrees was chosen because this is close to the actual value of the wind angle of the specimens tested in the lab. As before, the results for these tests came from the average values of the midline nodes of the system. The resulting relationship shows another linear relationship between strain and internal pressurization with an increase in strain as latex thickness decreases (Figure 18). From these results it can also be seen that by decreasing the latex thickness by 50% (1.25mm to 0.65mm), there is an order of magnitude increase in strain (0.04 to 0.12). This shows a very strong relationship between latex thicknesses and the amount of strain that can be expected from the system.

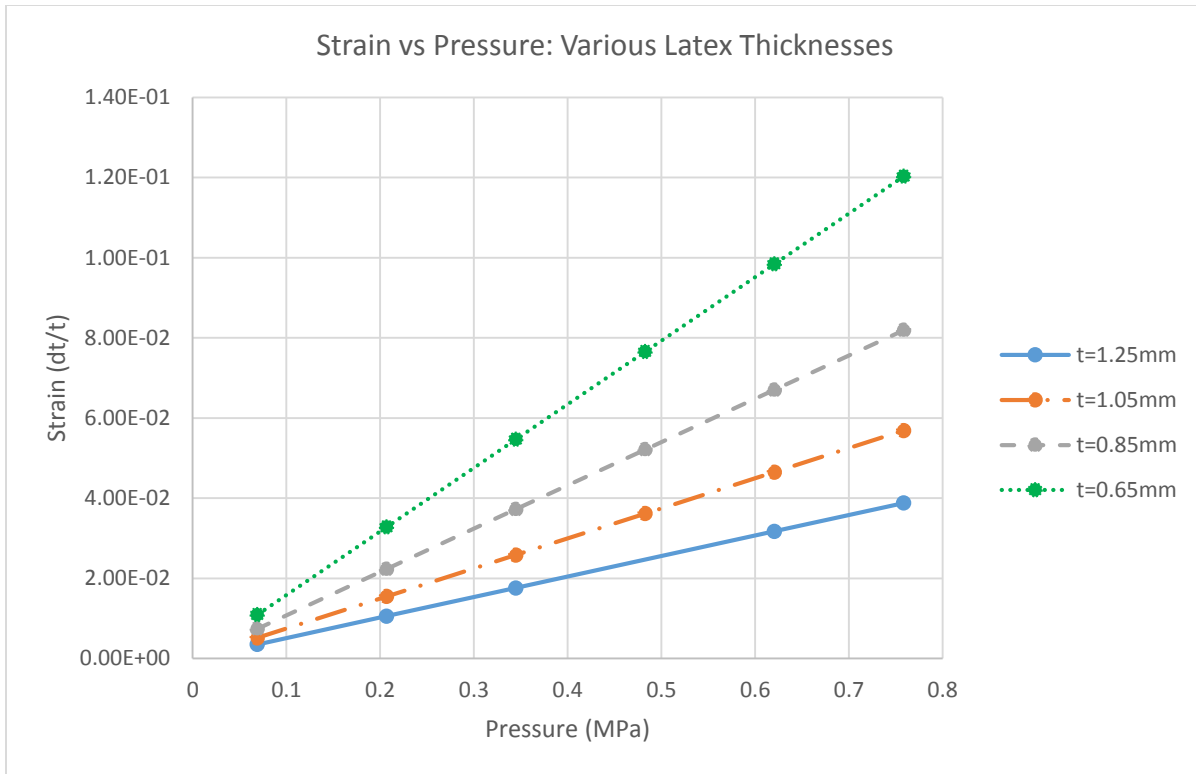


Figure 18: Strain vs Internal Pressurization for different values of Latex Thickness

3.2 Model under Transverse Loading

3.2.1 Model Setup

After completing free displacement tests, a second model was used to explore the effects of having a compressive force on top of the system (as would be the case in a socket loaded by a residual limb). The same geometry and boundary conditions were used for this model as the one for free displacement in Section 3.1 (Figure 12 and Table 4). However, a new load was added to the top square face of this model (Figure 19). The pressure load applied to this surface was modeled at various pressures to examine the response of the system for different levels of loading.

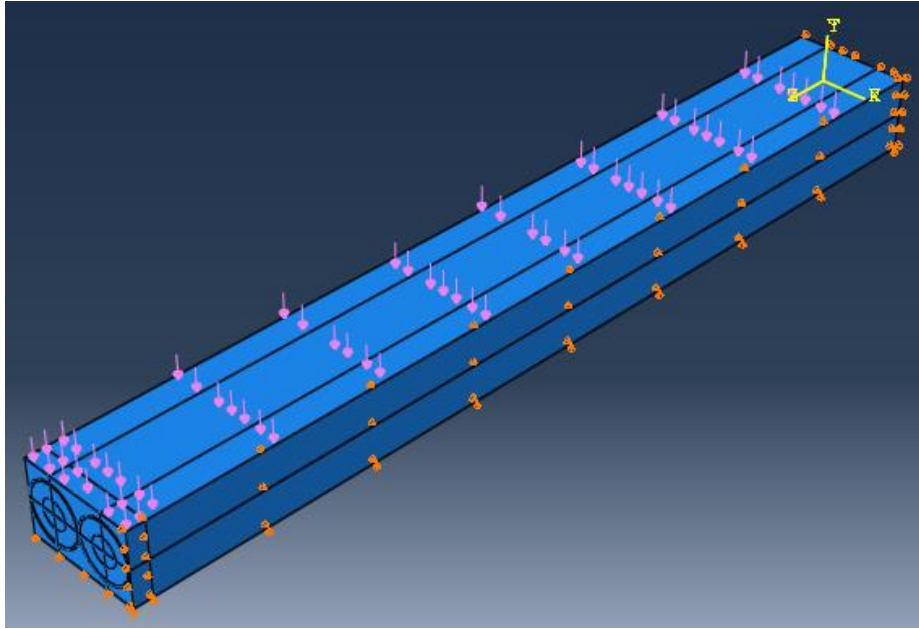


Figure 19: Top loaded multiple tube system

In addition to the boundary conditions used in previous investigations, a second boundary condition case was investigated with this model in which both sides of the system were constrained ($U1=0$ on both surfaces) to simulate a pocket in a socket that would keep both sides from expanding outward. Comparisons between these two cases of one side constrained versus two sides constrained were used to gain insight into how the system would differ from experimental testing once placed inside the pocket within the socket. The code for this model is included in Appendix B.

3.2.2 Model Results

For this model, the first test done was to determine the effective passive stiffness of the system. To do this, a pressure was applied to the top of the system and the internal pressure inside the tubes was set to zero.

Here, the stress in the figure is defined as force applied over the surface of the model in the transverse direction and the strain is defined as the change in thickness with respect to thickness. Since the system contains different materials at different volume fractions, these variables do not represent the actual internal stresses and strains but are used to provide a means to compare the effective properties of the system.

This passive stiffness test was done for both boundary conditions, and the results show an effective stiffness of about 2 MPa when one side of the system was constrained, and 4 MPa when both sides were constrained (Figure 20). When both sides of the system are constrained, expansion cannot occur on the sides, so a larger deformation through the thickness occurs and there is a larger effective stiffness.

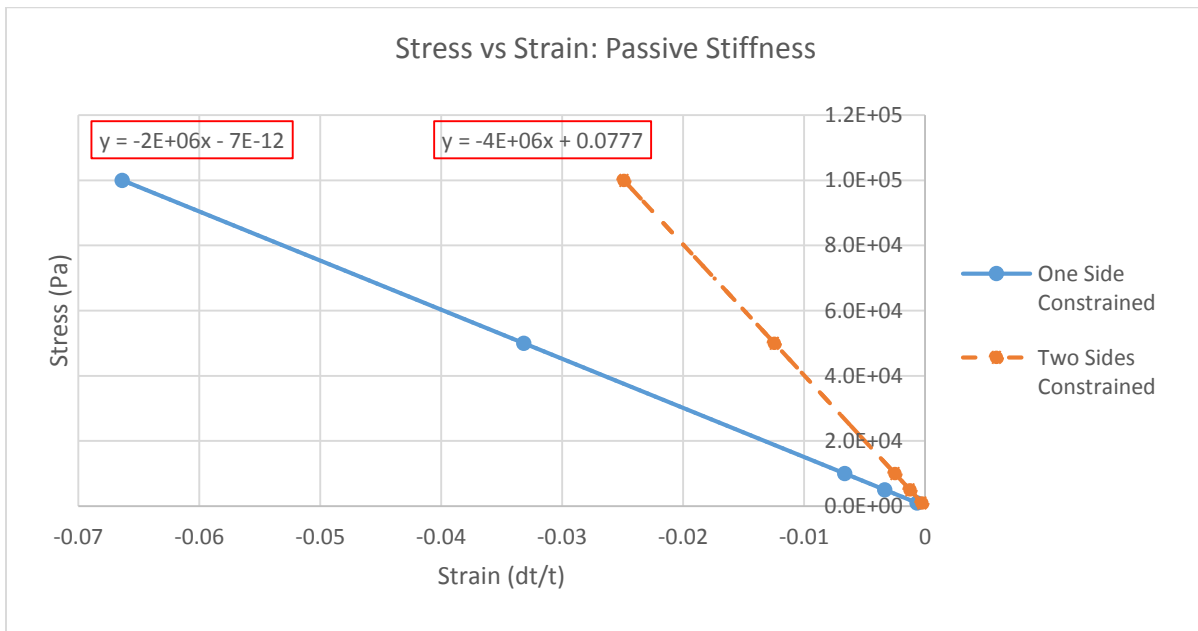


Figure 20: Stress vs strain for passive stiffness with two different boundary conditions

To examine this system further, the effective stress strain relationship was explored when the system was loaded from a top surface force and also had an internal pressure applied to the tubes. This condition represents the system under loading in a socket when the tubes are pressurized. As the top pressure on the system was increased, the average displacement of the midline of the system was recorded for various levels of internal pressurization 68.9, 206.8, 334.7, and 482.6 kPa (10, 30, 50, 70psi). The resulting relationships were plotted for both boundary conditions, one side constrained (Figure 21) and two sides constrained (Figure 22).

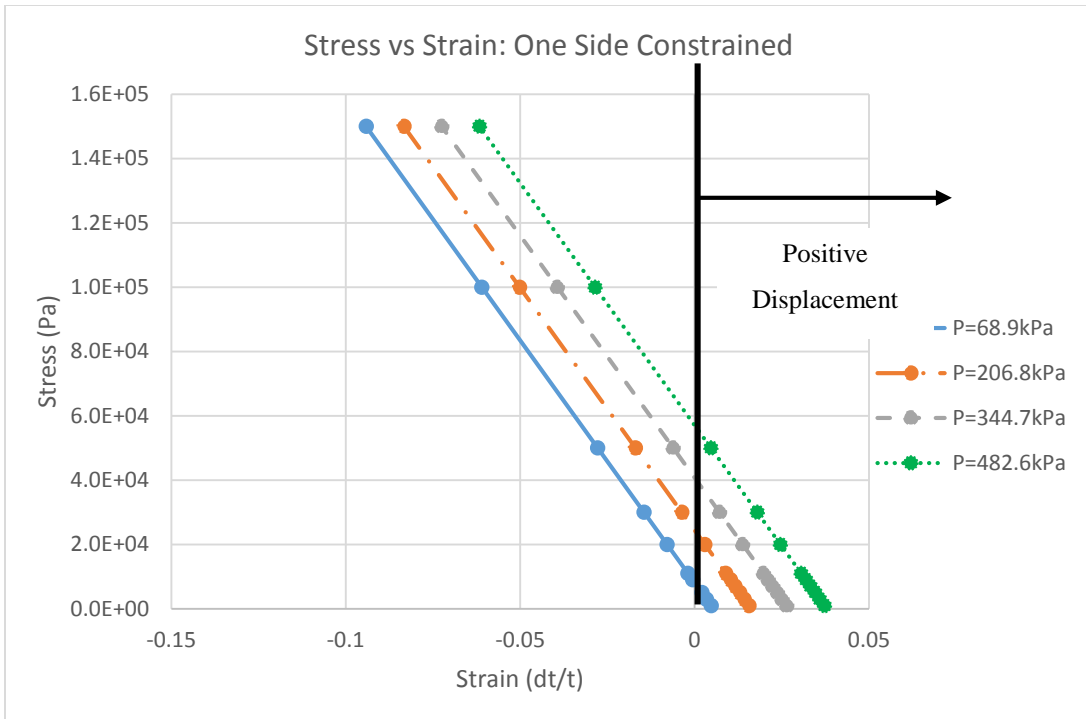


Figure 21: Stress vs strain relationship for top loaded model one side constrained

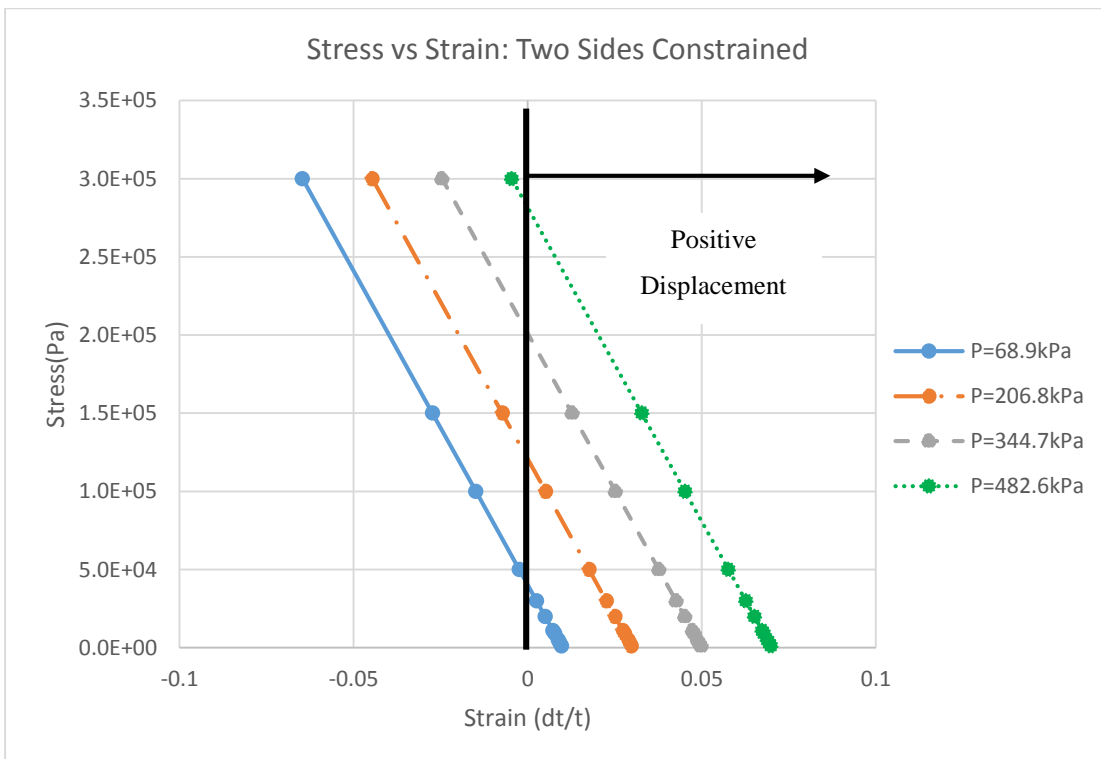


Figure 22: Stress vs strain relationship for top loaded model two sides constrained

From these two relationships it can be seen again that the modulus (slope) of the two sided constrained case is larger than one side constrained. Also as expected, at larger values of internal pressurization there is larger strain for the same value of stress, i.e. applied pressure. Additionally, these results express a linear relationship between the effective stress and strain in this system. These results will be compared to experimental results shown in Chapter 4.

Next, the effect of carbon fiber thickness was explored. For a wind angle of 30 degrees, an internal pressurization of 482.6 kPa (70 psi), and only one side of the system constrained, the top loading force was varied from 50-400 kPa to gather the resulting average of the displacement at the top surface of the midline (Figure 23).

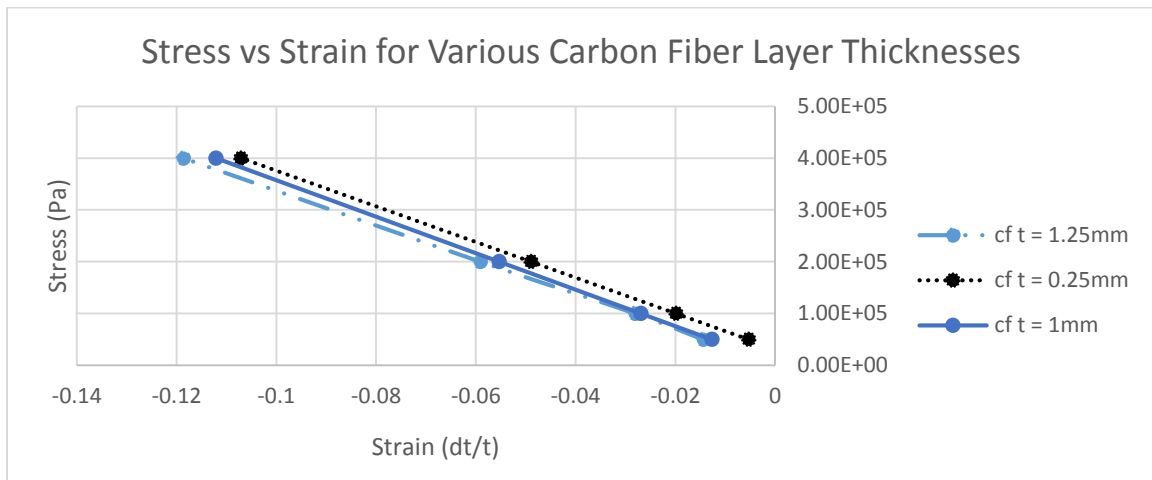


Figure 23: Stress vs strain for various carbon fiber layer thicknesses

These results express that the thickness of the carbon fiber layer has a very small effect on the overall displacement of the system. The difference in between a 1 mm and 0.25 mm thick carbon fiber layer is almost negligible which suggests that this parameter may not be of great importance.

Similar to free displacement (strain), the blocking force (stress) is an important characteristic that defines the maximum force that the actuator can produce for a given pressure. The blocking force versus pressure can provide a mechano-pressure coupling factor that can be valuable for describing the output response of the actuator. Knowing the passive stiffness and mechano-pressure coupling values, the response of a linear smart material can be fully characterized. To characterize a linear actuator fully the following relationship can be used:

$$\sigma = K\varepsilon + K_c P$$

where K and K_c are constants and $\varepsilon \sim \frac{\Delta L}{L}$ and $P \sim \frac{F}{A}$. Setting $\varepsilon = 0$ for this blocked force case, the constant K_c can be found from the relationship of internal pressure and block stress. Shown in Figure 24 are the block stresses for increasing pressure, resulting in a mechano-pressure coupling of 0.0041 and 0.0201 for the one side and two side systems respectively. It can be seen that there is a linear relationship between internal pressurization and the amount of force required to cause zero deflection of the top of the system. Additionally, a larger blocking force is produced in the system where both sides are constrained. This shows that in a system like the socket, this material generates a stronger force than the experimental case outside the socket where the sides can move.

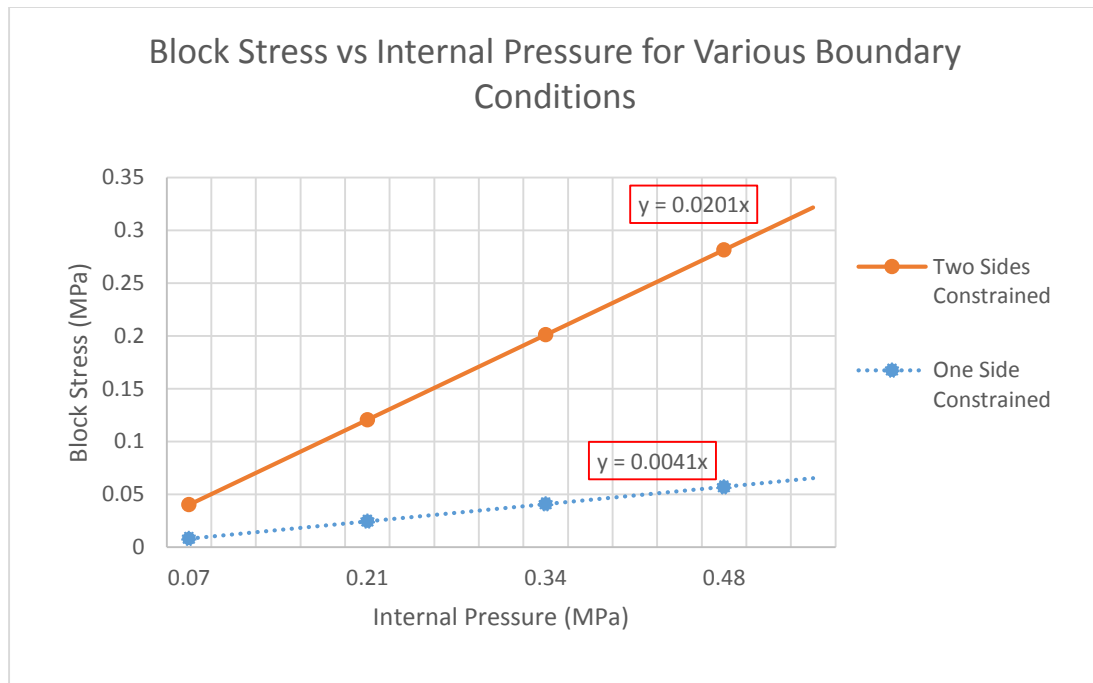


Figure 24: Blocking stress vs internal pressurization for various boundary conditions

Along with the displacement experienced by the system, the maximum stresses in the actuators caused by loading and pressurization in the worst case scenario was of interest. A pressure load of 855.4269 kPa was applied to the top surface of the system to simulate the full weight of a 250 lb person, and the tube was pressurized to 689.5 kPa (100 psi). In this case, the largest stresses were found at a critical section in the carbon fiber tube closest to the end cap. The maximum von mises stress was about 52.9 MPa. Using a cylindrical coordinate system, the

maximum radial, circumferential, and longitudinal stresses at this location were found to be about 12.1 MPa, 11.0MPa, and 39.0MPa respectively. From these results, the system will not fail because the yield strength of carbon fiber is on the order of 100MPa. Considering this and that only a fraction of the total weight of a patient will be on this system, the stresses are not expected to cause failure. Figure 33, Figure 34, Figure 35, and Figure 36 in Appendix A show the stresses on the top surface and outer end cap of the system.

CHAPTER IV: EXPERIMENTAL DATA

Experiments were conducted for multiple f2mc wafers for comparison and validation with the model results previously discussed in Chapter 3. The fabrication of the wafers, experimental setup, and experimental results are discussed in this chapter. The wafers are also analyzed for their proficiency in compensating for residual limb volume change.

4.1 F2mc Fabrication

To create f2mc wafers for testing, four components are needed: a latex rubber tube, a carbon fiber braided sheath, a pourable urethane rubber, and a fitting for pressurization. First, the latex rubber tube is inserted into the carbon fiber braided sheath. One end of the carbon fiber sleeve and tube is sealed, and the sleeved tube is then wound into the desired shape, such as a circular spiral. Afterwards, the carbon fiber sleeve is wetted using a urethane mixture of Vytaflex[®] 20 from Smooth-On, Inc., which also helps hold the shape. After curing, barbed male fittings are epoxied onto the open end of the spiral. A female fitting with a push-to-connect end is threaded onto the male fitting to ensure a tight seal for pressurization. Figure 25a/b show a wafer before and after attachment of fittings, and Figure 25c shows an elongated wafer shape.

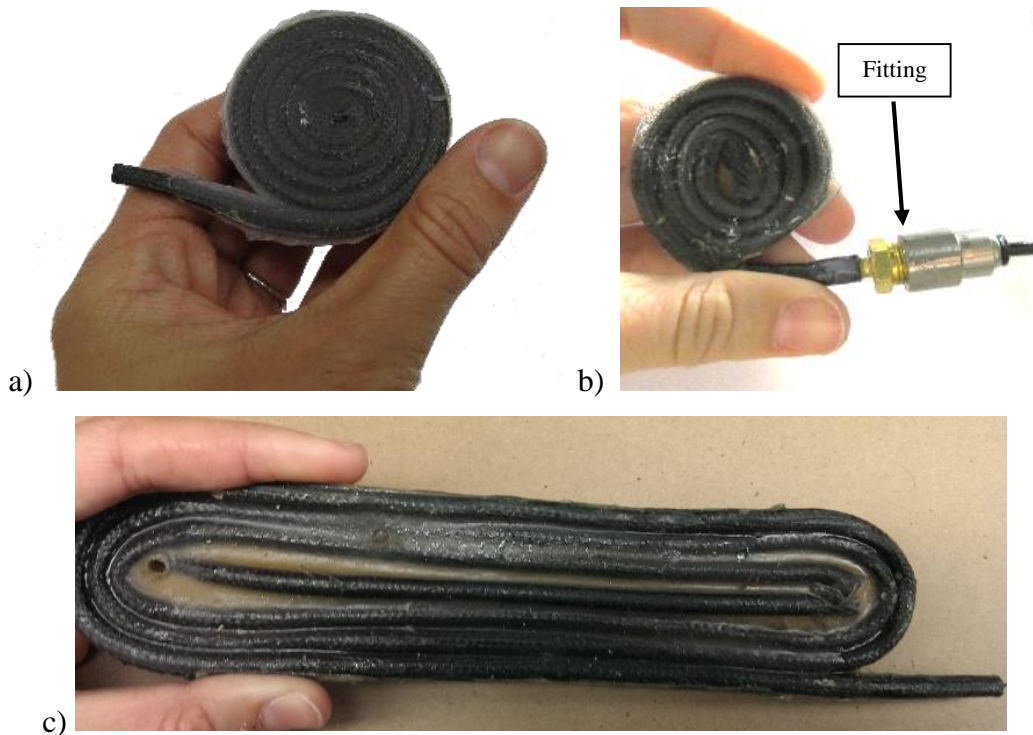


Figure 25: a) Small f2mc circular wafer before a fitting is applied, b) Small f2mc circular wafer after a fitting is applied, c) Larger elongated f2mc wafer

In the following experimental tests, one small circular wafer and one larger elongated wafer were tested. Information about these wafers can be found in Table 5.

Table 5: Wafers used in Experimental Testing

	Surface Area	Approximate Initial Wind Angle	Thickness
Large Elongated Wafer	34600 mm^2	30°	8.8 mm
Small Circular Wafer	28.96 mm^2	40°	5 mm

4.2 Experimental Setup

In the experiment, two sample wafers (one large and one small) were placed one at a time between two aluminum plates in an ADMET testing frame with a load cell and compression plate controlled by an MTEST Quattro software pack (Figure 26). The top and bottom surfaces of the wafer were coated with petroleum jelly to allow sliding along the compression plates. A regulator was used to control the amount of air pressure coming into the wafer, and a pressure transducer was used to measure the exact value of pressure (the specifics of all equipment used are included in the Appendix in Table 9).

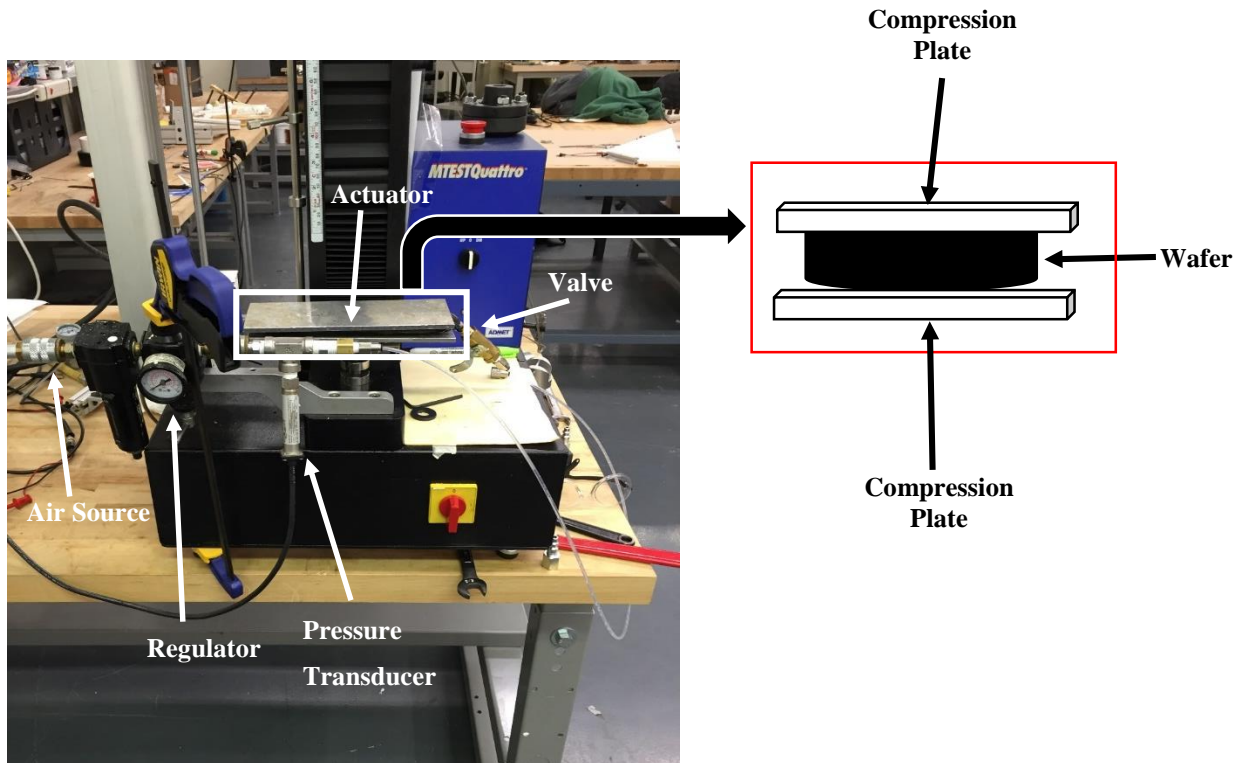


Figure 26: Experimental setup for compression testing of f2mc wafers

A Fluke Multimeter was used to display the signal voltage from the pressure transducer to ensure an exact pressurization value. The conversion from voltage to pressure for the pressure transducer is as follows:

$$P = ((V - V_i) * 500)$$

where V_i is the initial voltage read out with zero pressure, and P and V are pressure and voltage in psi and volts respectively. The sensitivity of the pressure transducer is 500 psi/Volt.

The objective of these experiments was to fully characterize the wafers with different levels of internal pressurization similar to Figure 21 from the finite element model. Therefore, in these experiments, we began with free displacement ($F=0$) and applied an increasing compressive load until a maximum load of about 1 kN was achieved. The process was then repeated for different internal pressures.

The steps in the process for testing each sample wafer were as follows:

1. Bring the load cell down to rest on the top plate above the sample, until it touches the surface without applying any load
2. Set as the Home Position
3. Zero the load (0 N preload)
4. Move the load cell away from the sample
5. Adjust the pressure in the sample, using the regulator and readout from the multimeter, to the desired pressure value
6. Move the load cell to the Home Position while measuring the load at 1000 samples per second
7. Continue to load the sample to 110 lbs at 300 samples per second
8. Repeat steps 4-7 for pressures ranging from 0-482.6 kPa (0-70psi) in increments of 34.5 kPa (5psi) two times for each pressure step on each wafer (a total of four tests at each pressure)

4.3 Experimental Results

The data for force on the load cell from one of the larger actuator trials was recorded as a function of the displacement of the actuator. The force was converted into stress by dividing the load value from the load cell by the area of the wafer, and the displacement was divided by the thickness of the wafer to provide strain in the thickness direction (Figure 27). These results show

that greater force production and a larger displacement occurs at higher pressures as expected. These tests also show the largest displacement of an actuator with no load ($x=0$). At the highest pressure (70 psi), the maximum strain was about 98% with no load on top of the system.

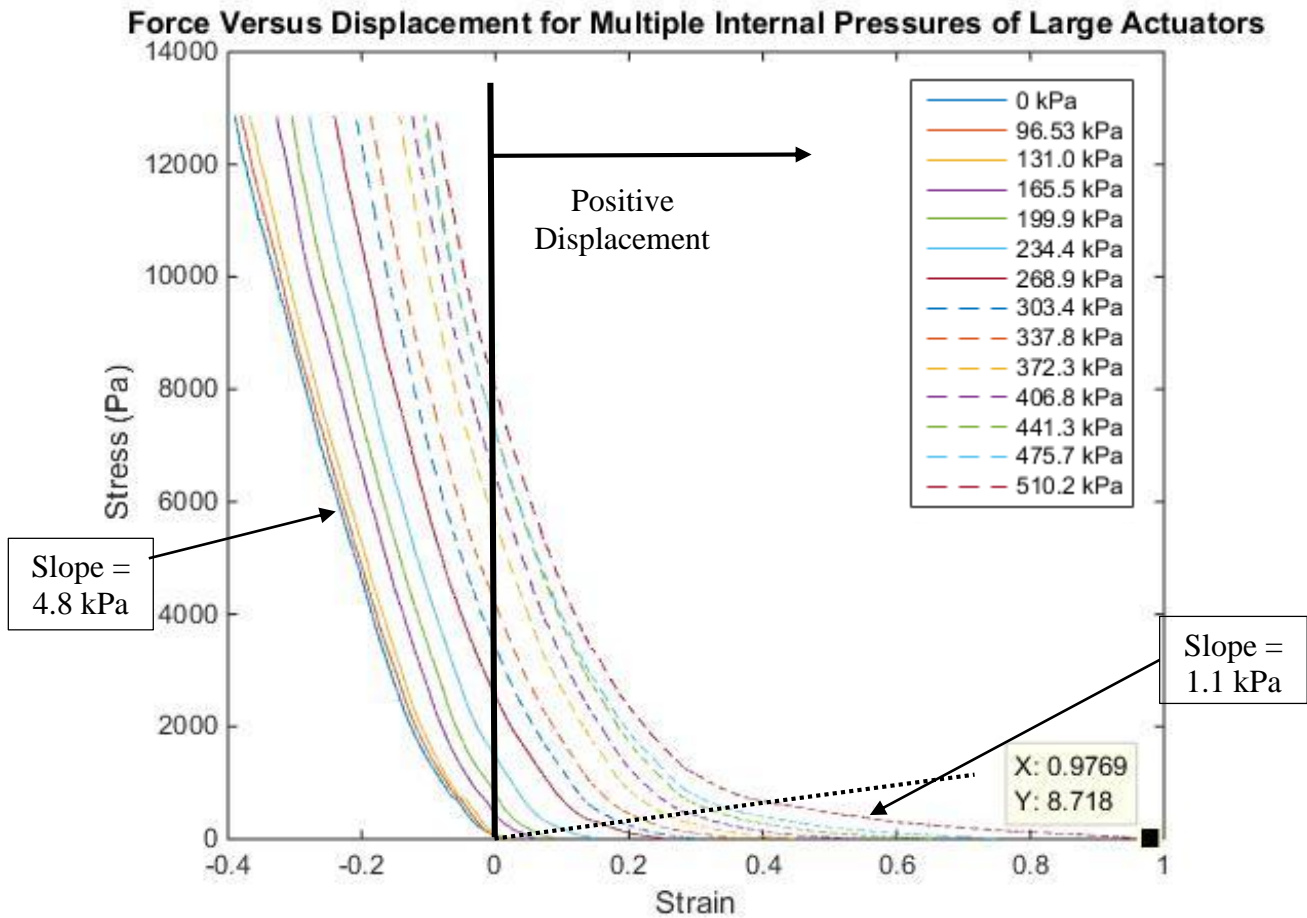


Figure 27: Stress vs strain relationship for experimental results of the large wafer

The results shown in Figure 27 express that the actuators are nonlinear, unlike the results predicted by the finite element model. The results show that the wafer transitions from a soft region under small load (slope= 1.1 kPa) to a stiff region under larger loads (slope=4.8 kPa). This transitional region is approximated by the black dotted line, which shows a strong relationship with applied pressure. This could be beneficial for use within prosthetic sockets because stiffness can be controlled during use. The wafer can be controlled to be stiffer or softer depending on the patient's needs throughout the day. Another impressive characteristic of the wafer shown here is its ability to achieve nearly 100% strain in the thickness direction.

In comparing the finite element model discussed earlier to these results, the experimental results express a significantly higher strain than the model results where only one side is constrained (Figure 21). Additionally, the modulus calculated from the linear region of the experimental stress vs strain relationship was found to be about 4.8 kPa. This is three orders of magnitude smaller than the model's effective modulus of 2 MPa. As a result, the stiffer model yields much less strain than the actual system in the experimental tests.

A smaller wafer was also tested to see how the size and configuration may affect the performance of the system. Figure 28 below shows one smaller circular wafer and one larger elongated wafer. These different shapes show some of the options for placing wafers within the socket in whatever size and shape is needed at different pressure points.



Figure 28: Different sizes of f2mc wafers tested

The results curve for this smaller actuator shows much lower strain at the same stress given for the larger actuator. From these results, it can be seen that the largest achievable strain through the thickness at 482.6 kPa (70psi) is only about 54% (0.5362) instead of 98% found in the larger wafers. One reason for this difference may be the wind angle of each wafer. The tighter spiraled small circular wafer has a larger wind angle which reduces the maximum achievable strain.

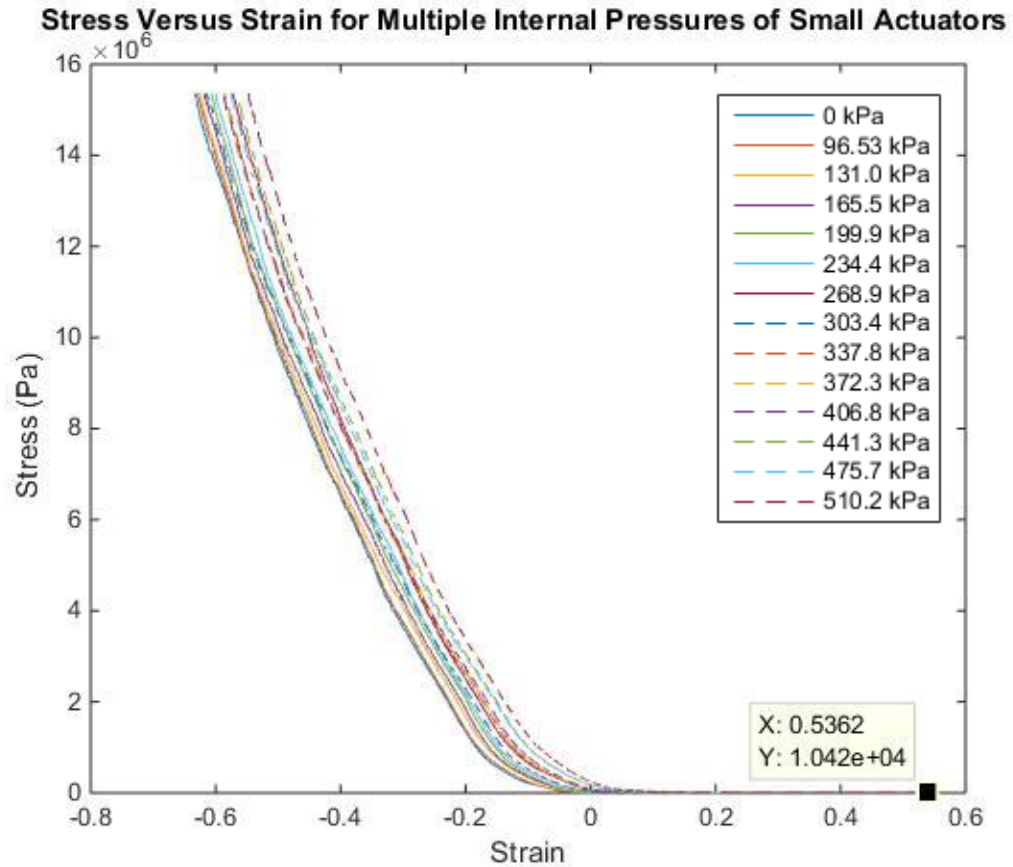


Figure 29: Stress vs strain relationship for experimental results of the small wafer

To continue exploring the effectiveness of the small wafers next to the larger ones, the displacement of the top surface of the system was measured as a function of the internal pressure of the tubes when the top surface was free to move (Figure 30). These results show a displacement as high as 8.6mm for the larger wafer, which is a significant displacement considering the thickness of the wafer is only about 8.8 mm. The maximum displacement for the smaller wafer was about 2.0 mm, which is still significant. Although the smaller circular wafers provide less displacement, they may still be useful for a patient. These wafers can be tailored for each individual patient's requirements for size and shape. Because of this desired tailorability, both small and large wafers are useful and can provide support and significant displacement.

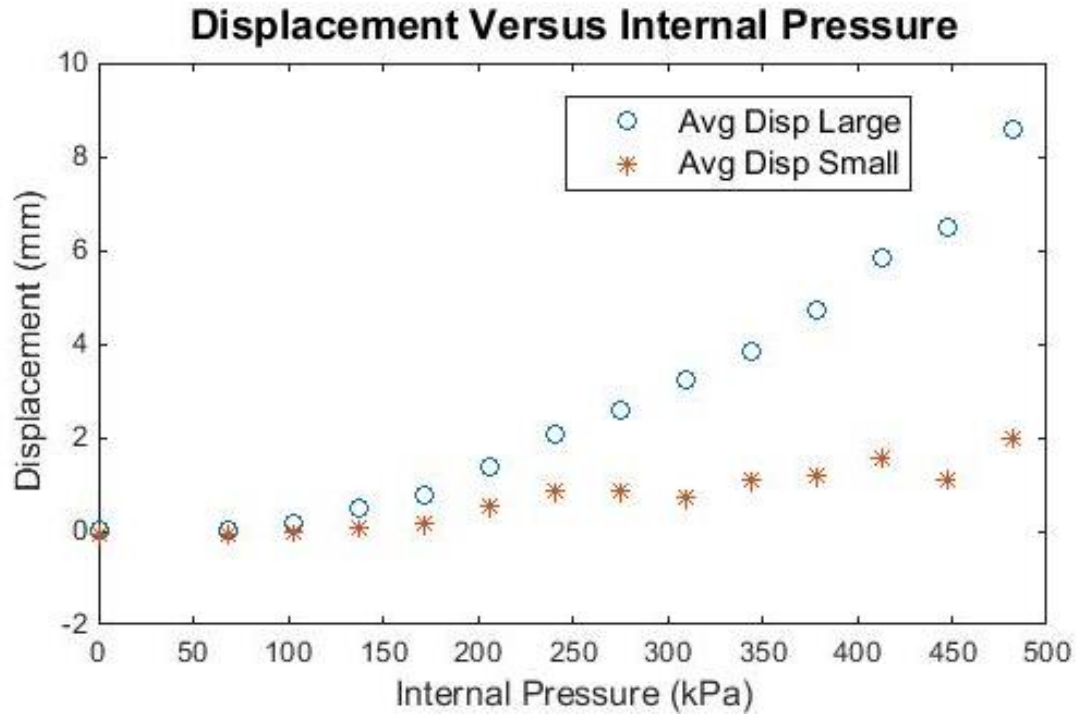


Figure 30: Free displacement vs internal pressure for Wafer 1 (large) and Wafer 2 (small)

To determine if this 8.6 mm displacement from the larger actuator was sufficient for the volume compensation needed in a residual limb, some assumptions were made to model the residual limb geometry. Assuming the residual limb can be modeled as a perfect cylinder with a hemisphere on the bottom, estimates were made for the dimensions to see how much volume change compensation was needed from the actuators (Figure 31). A maximum circumference of a transtibial (below knee) residual limb of about 50cm (radius $r = 7.96\text{cm}$) and a height (h) of 20 cm from knee to the tip of the stump. The volume was calculated using the equation for a hemisphere on top of a cylinder:

$$Vol = \pi r^2 h + \frac{2}{3} \pi r^3$$

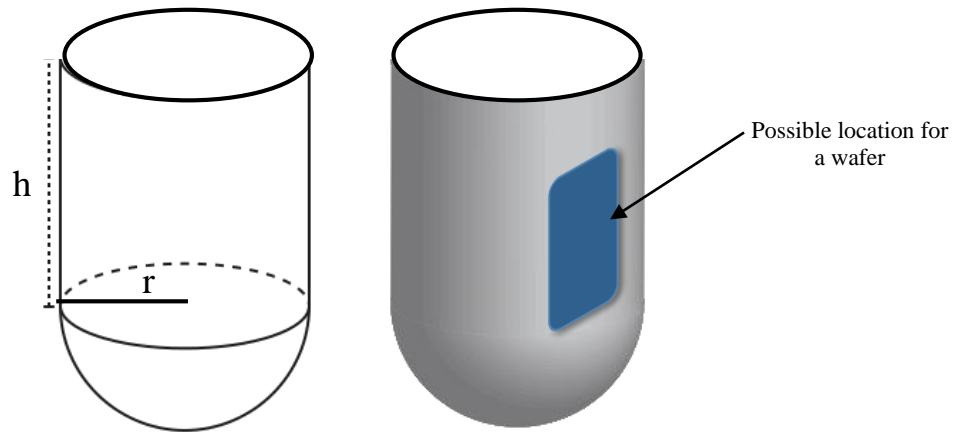


Figure 31: Residual limb model for volume change

Using this equation, the volume of the residual limb was estimated to be 5034.3 cm^3 . Rounding to 5100 cm^3 to account for any deviations from a perfect cylinder/hemispherical model, the maximum expected volume change is 11% of this value. That means the wafers in the socket would need to account for 561 cm^3 of volume change. Assuming that the displacement of 8.6mm on the surface of the actuator was uniform across the entire surface, the volume was estimated with the following equation:

$$Vol = A * u$$

where A is the area of the top surface of the actuator (346.496 cm^2), and u is the displacement of the top surface. The volume of protrusion of the actuator was found to be 297.987 cm^3 . This shows that one wafer can account for over half of that total residual limb volume change.

In the final application of these wafers, more than one would be placed within the socket at different locations of volume change. These wafers should produce an adequate amount of volume change for the patient.

Figure 32a shows an example of a patient's socket that has an area mapped out where an elongated wafer would be placed to compensate for frequent volume change. Socket maps similar to this one would be used to attain the exact desired size and shape of each wafer needed for each individual patient. Figure 32b shows an example of how multiple wafers could be placed inside a socket.



Figure 32: a) Identified areas of critical volume change from a patient at the VA Medical Center in Richmond, VA, b) elongated wafers integrated into a socket

CHAPTER V: CONCLUSIONS AND FUTURE WORK

5.1 Conclusions

To manage volume change in a residual limb, several factors are important for an amputee: when to put on the first prosthetic socket, when a new socket is required, and the design of the socket itself [2]. The timing to put on the first prosthetic socket depends largely on gaining control of the residual limb volume. With an earlier first socket, patients tend to have a more normal gait, independent lifestyle, higher physical activity level, and better psychological stability. The goal of the f2mc system presented here is to provide an earlier fit time for amputees, and help facilitate a more comfortable state during daily usage.

Through experimentation, it has been found that f2mc wafers can provide at least 8.6 mm of displacement which should successfully reduce the discomfort felt within a socket due to residual limb volume change. Multiple wafers would be placed around the socket to provide support in any area that experiences shrinking. This system would also work for cases where the residual limb expands instead of shrinks. The tubes would not be pressurized, but would provide support as the residual limb expands onto them.

The linear finite element model created here is a first step in the analysis and design of the system. Through this model, it was found that latex thickness and wind angle have the largest effect on the magnitude of displacement of the system. However, the magnitudes for strain found in the model are much lower than those found in the experimental results. The hypothesized reason for this difference is that the linear model cannot capture the geometric and material nonlinearities that are present in the physical system. It is also difficult to capture the braided sleeve of the carbon fiber tube perfectly. Some final improvements to this model would be to simulate a physical fluid moving through the system instead of just a pressure load inside the tubes, and a non-static loading force as well.

Overall, through the experiments and finite element results presented here, this f2mc system is predicted to be a good improvement to prosthetic sockets to reduce the effect of residual limb volume change. Initial results show that the displacement of the wafers will be significant and that they can support loads much higher than those likely to be found in a prosthetic socket. This solution is a viable alternative to those currently on the market particularly for its ability to

be easily adapted to each patient's need, and incorporate both volume reduction and expansion. It also presents improvement in the area of over-inflation. In the full implementation of this system, a control loop would be included to activate pressurization whenever there is a loss of contact between the residual limb and the socket. This control system would ensure that the patient could not inflate the system themselves to the point of causing tissue injury.

5.2 Future Work

The next step for this research includes much more experimental testing. Experimental testing needed includes: cyclic fatigue testing of the actuators, variation of the working fluid, in-socket measurements of stress and strain, clinical trials of patients wearing the actuator filled sockets, and comparison with a vacuum system.

1. Fatigue testing will be important because the actuators in this application will experience continuous loading throughout the day as the amputee stands and moves.
2. Testing various working fluids for pressurization will help explore the effect of the working fluid, and will lead to optimization of the pressurization method by finding which fluid creates the most displacement and support.
3. Measuring the strain of the actuators in the socket will help to confirm what the finite element model already predicts: that more displacement will occur in socket with both sides constrained.
4. By having patients walk with the actuators in their socket, valuable information will be gained about the stresses on the system, and how much load is actually being applied on each actuator from the residual limb.
5. Lastly, comparing this system side by side with the currently used vacuum pump system will help to show that this system is indeed superior in providing comfort.

Another important step for this project will be to create a non-linear finite element model. Through the work discussed here, it was found that the non-linearity of the material and geometry of this system may be incredibly important. The linear model was useful for manipulating variables and taking a first attempt at modeling the system. Through this model however, it is clear that the system needs to be modeled as non-linear to accurately represent how much displacement is occurring. Another improvement to this model will be non-static loading. For a preliminary model, a static load only was applied to compare to experimental testing on the wafers

themselves. In the future, it will be important to test the system under a walking or running loading situation to better simulate the patients' use of the system.

Some developments to the system also include developing a feedback control system instead of using manual pressurization. Currently for testing purposes, the system is controlled by manually applying more or less internal pressure to the tubes. The final solution in the socket would need a feedback system that can sense when more or less pressurization is needed in the tubes. Any changes in pressure measured by pressure or force sensors would be used to send a signal to the control system to regulate volume of the wafer. These system would be beneficial for most patients, especially those with loss of sensation in the limb due to other health problems such as diabetes.

REFERENCES

1. Ziegler-Graham, K., et al., *Estimating the Prevalence of Limb Loss in the United States: 2005 to 2050*. Archives of Physical Medicine and Rehabilitation, 2008. **89**(3): p. 422-429.
2. Sanders, J.E. and S. Fatone, *Residual limb volume change: Systematic review of measurement and management*. J Rehabil Res Dev, 2011. **48**(8): p. 949-986.
3. Mishra, R. *Amputation Rate for US Troops Twice That of Past Wars*. Boston Globe, 2004.
4. Reiber, G.E., et al., *Servicemembers and veterans with major traumatic limb loss from Vietnam war and OIF/OEF conflicts: Survey methods, participants, and summary findings*. Journal of rehabilitation research and development, 2010. **47**(4): p. 275-298.
5. Greenwald, R.M., R.C. Dean, and W.J. Board, *Volume management: Smart Variable Geometry Socket (SVGS) technology for lower-limb prostheses*. JPO: Journal of Prosthetics and Orthotics, 2003. **15**(3): p. 107.
6. Board, W., G. Street, and C. Caspers, *A comparison of trans-tibial amputee suction and vacuum socket conditions*. Prosthetics and orthotics international, 2001. **25**(3): p. 202-209.
7. Fernie, G. and P. Holliday, *Volume fluctuations in the residual limbs of lower limb amputees*. Archives of Physical Medicine and Rehabilitation, 1982. **63**(4): p. 162.
8. Sanders, J.E., E.L. Rogers, and D.C. Abrahamson, *Assessment of residual-limb volume change using bioimpedance*. Journal of Rehabilitation Research & Development, 2007. **44**(4).
9. Portnoy, S., et al., *Real-time subject-specific analyses of dynamic internal tissue loads in the residual limb of transtibial amputees*. Medical engineering & physics, 2010. **32**(4): p. 312-323.
10. Portnoy, S., et al., *Real-time patient-specific finite element analysis of internal stresses in the soft tissues of a residual limb: A new tool for prosthetic fitting*. Annals of Biomedical Engineering, 2007. **35**(1): p. 120-135.
11. Call, D., C. Coulter, and S. Nicely, *Discussions on prosthetics and ways to improve the fit and comfort for the amputee at Virginia Prosthetics*, M. Philen and M. Madigan, Editors. 2010: Roanoke VA.
12. Lovegreen, W., *Personal communication with William Lovegreen at VA Medical Center*, M. Philen and M. Madigan, Editors. 2013.

13. Portnoy, S., et al., *Internal mechanical conditions in the soft tissues of a residual limb of a trans-tibial amputee*. Journal of biomechanics, 2008. **41**(9): p. 1897-1909.
14. Zhang, M., et al., *Clinical investigation of the pressure and shear stress on the trans-tibial stump with a prosthesis*. Medical engineering & physics, 1998. **20**(3): p. 188-198.
15. Faustini, M.C., R.R. Neptune, and R.H. Crawford, *The quasi-static response of compliant prosthetic sockets for transtibial amputees using finite element methods*. Medical Engineering and Physics, 2006. **28**(2): p. 114-121.
16. Love, M.G., *Prosthetic socket containing inflatable means*. 1995, Google Patents.
17. Cochrane, H., K. Orsi, and P. Reilly, *Lower limb amputation Part 3: Prosthetics-a 10 year literature review*. Prosthetics and orthotics international, 2001. **25**(1): p. 21-28.
18. Sanders, J.E., et al., *Testing of elastomeric liners used in limb prosthetics: classification of 15 products by mechanical performance*. Journal of rehabilitation research and development, 2004. **41**(2): p. 175-186.
19. Sanders, J.E., et al., *Effects of elevated vacuum on in-socket residual limb fluid volume: Case study results using bioimpedance analysis*. Journal of rehabilitation research and development, 2011. **48**(10): p. 1231.
20. Ottobock, *Below-knee prosthesis with: Triton Harmony*. 2013.
21. Philen, M., et al. *Variable stiffness adaptive structures utilizing hydraulically pressurized flexible matrix composites with valve control*. in *47th AIAA/ASME/ASCE/AHS/ASC Structures, Structural Dynamics and Materials Conference*. 2006. Newport, RI, United States: American Inst. Aeronautics and Astronautics Inc.
22. Philen, M.K., et al., *Fibrillar network adaptive structure with ion-transport actuation*. Journal of Intelligent Material Systems and Structures, 2007. **18**(4): p. 323-334.
23. Shan, Y., et al., *Variable stiffness structures utilizing fluidic flexible matrix composites*. Journal of Intelligent Material Systems and Structures, 2009. **20**(4): p. 443-456.
24. Liu, W. and C.R. Rahn, *Fiber-reinforced membrane models of McKibben actuators*. Transactions of the ASME. Journal of Applied Mechanics, 2003. **70**(6): p. 853-9.
25. Hyer, M.W., *Stress Analysis of Fiber-Reinforced Composite Materials*. 2009, Lancaster, Pennsylvania: DEStech Publications, Inc.
26. Bakis, C., *Flexible Matrix Composite Skins for One-dimensional Wing Morphing*. Journal of Intelligent Material Systems and Structures, 2010. **21**: p. 1771-1781.

APPENDIX A: FIGURES AND TABLES

Table 6: Material Properties for Composite Layup Validation

	Graphite-Composite	Aluminum
E11 (GPa)	155	72.4
E22=E33 (GPa)	12.1	
v12=v13	0.2248	0.3
v23	0.458	
G12=G13 (GPa)	4.4	
G23 (GPa)	3.2	

Table 7: Material Properties

	Carbon Fiber Matrix	Aluminum	Latex	VytaFlex® 20
E11 (GPa)	155	70	0.01	0.00103
E22=E33 (GPa)	0.00206			
v12=v13	0.389	0.33	0.48	0.499
v23	0.495			
G12=G13 (MPa)	0.644			0.0000322
G23 (GPa)	0.689			

Table 8: Tube Model Validation-Abaqus Results

Angle	FMC Only: End Cap Force	
	U3	dL/L
0	1.50E-03	1.50E-03
10	-2.33E-02	-2.33E-02
20	-1.01E-01	-1.01E-01
30	-2.42E-01	-2.42E-01
40	-3.56E-01	-3.56E-01
50	-1.65E-01	-1.65E-01
60	1.39E-01	1.39E-01
70	2.95E-01	2.95E-01
80	3.55E-01	3.55E-01
90	2.87E-01	2.87E-01

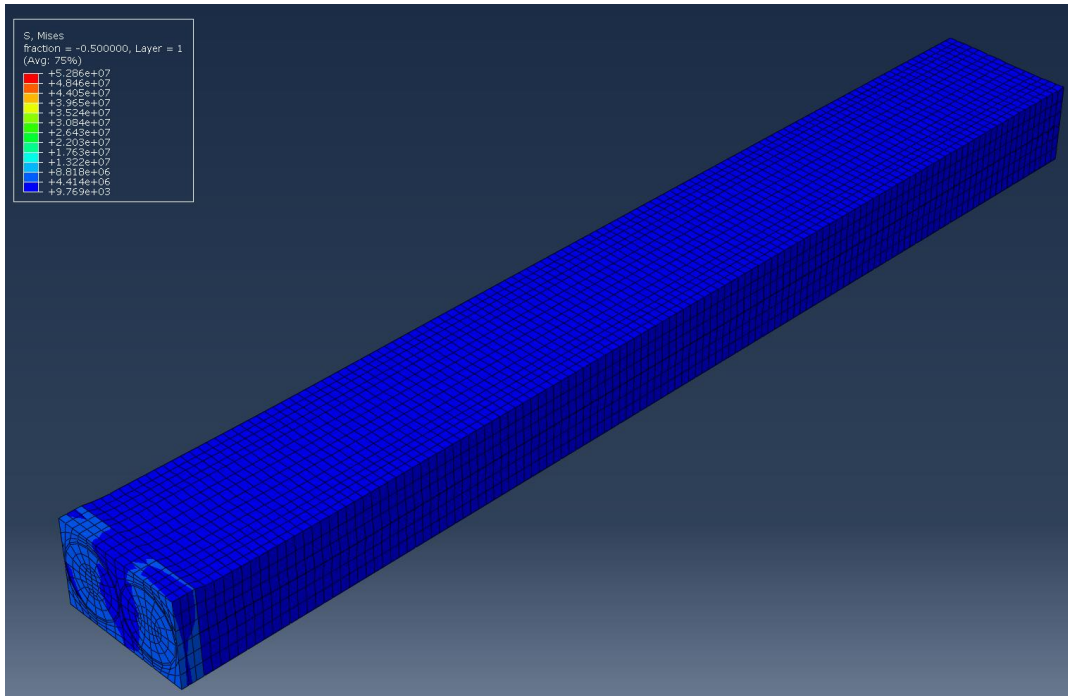


Figure 33: Von Mises Stresses with the load of a 250 lb person at internal pressure of 100psi

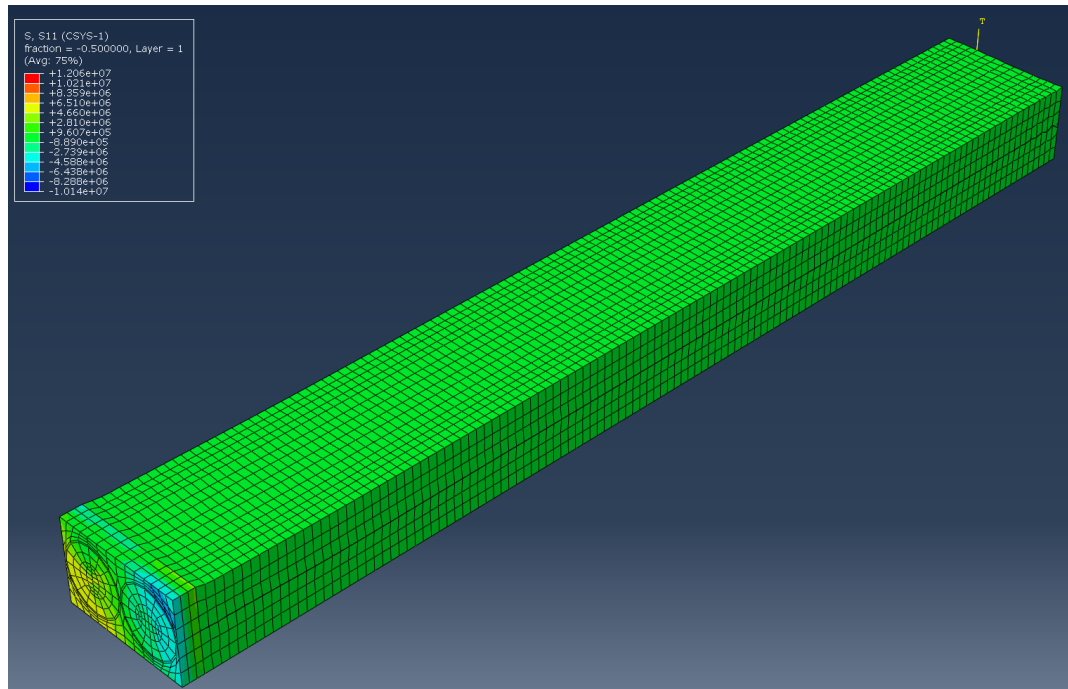


Figure 34: Radial Stress with the load of a 250 lb person at an internal pressure of 100psi

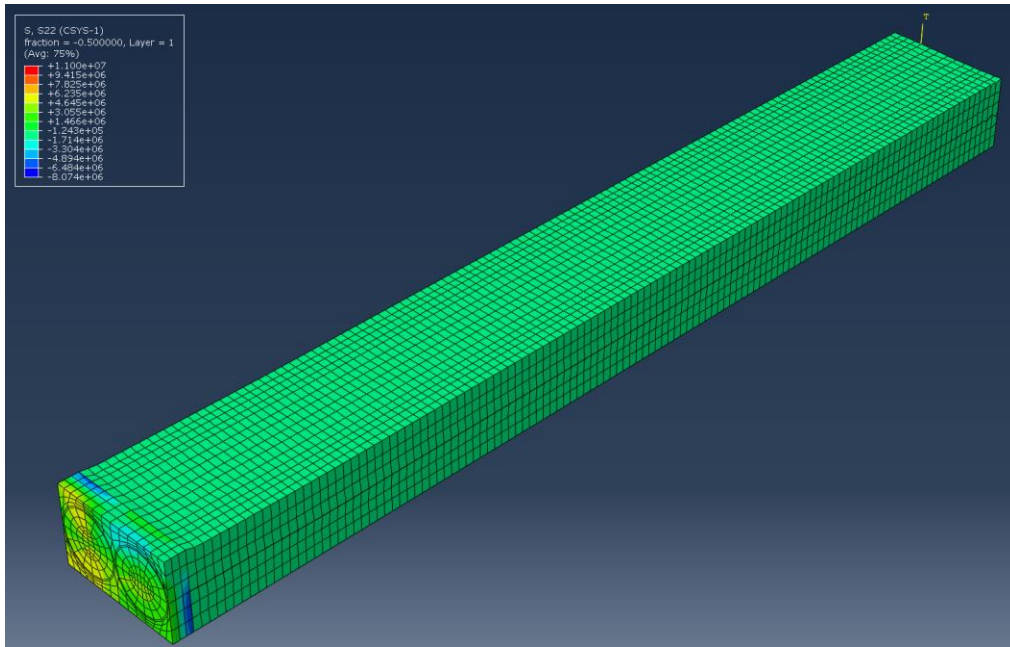


Figure 35: Circumferential Stresses with the load of a 250 lb person at an internal pressure of 100psi

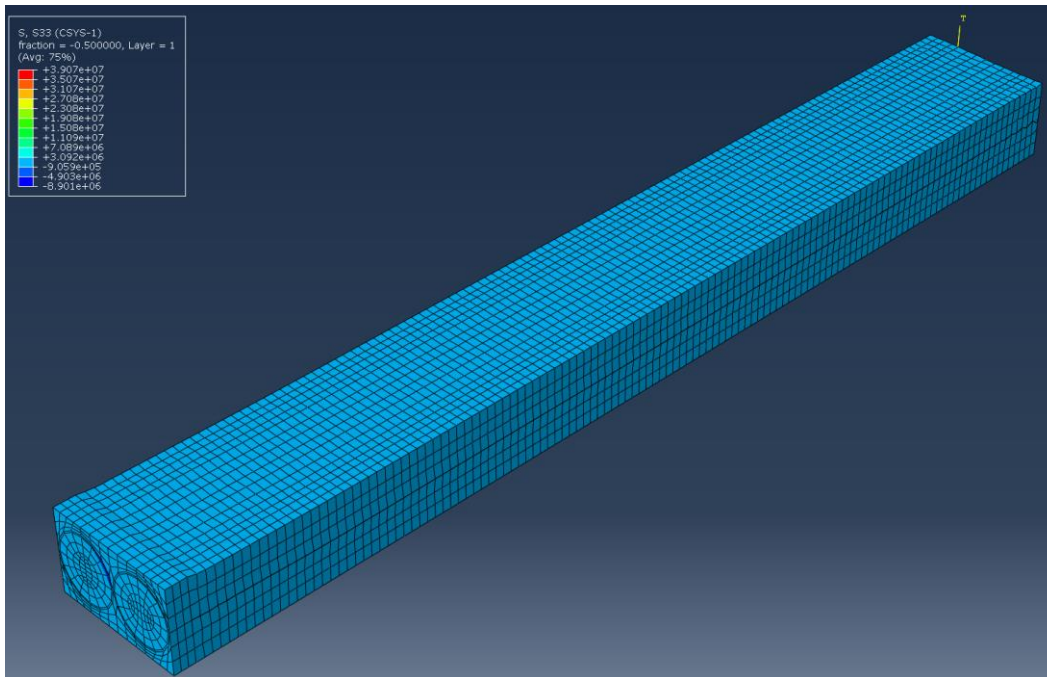


Figure 36: Longitudinal Stresses with the load of a 250 lb person at an internal pressure of 100psi

Table 9: Equipment Specifications for Wafer Experimentation

Pressure Transducer	AshCroft: Model # K15M0215F22000 Range: 2000 psi Accuracy: 0.5%
Pressure Regulator	Norgren: Model #R72G-2AT-RMG
Load Cell	Interface SM-1000 Serial Number: 626784
Multimeter	Fluke 115 True RMS Multimeter
Power Supply	Electro Industries Power Supply

APPENDIX B: CODE

AB1: Code used for tube model validation

```
%% Code for composite tube theoretical calculations
close all
clear all
E1=115e9;    %Pa
E2=2.06e6;   %Pa
G12=6.44e5;  %Pa
v12=0.389;
v21=v12*E2/E1;

Q11=E1/(1-v12*v21);
Q12=v21*E1/(1-v12*v21);
Q22=E2/(1-v12*v21);
Q66=G12;

R=0.00315;    % m
F=0;          % N
P=1e5;        % Pa
B=0;          % Pa
L=0.10;       % m

t=0.0002;    %m
h=t;
thetavec=linspace(0,90,100);
for jiter=1:length(thetavec),
    theta=thetavec(jiter);    %deg.

    angles=[theta, -theta];
    k=length(angles);
    h=t/k;    %thickness per each layer

    Q11=E1/(1-v12*v21);
    Q12=v21*E1/(1-v12*v21);
    Q22=E2/(1-v12*v21);
    Q66=G12;

    A11=0;
    A12=0;
    A22=0;

    for i=1:k
        m=cos(angles(i)/180*pi);
        n=sin(angles(i)/180*pi);
        Q11_bar(i)=Q11*m^4+2*(Q12+2*Q66)*n^2*m^2+Q22*n^4;
        Q12_bar(i)=(Q11+Q12-4*Q66)*n^2*m^2+Q12*(n^4+m^4);
        Q22_bar(i)=Q11*n^4+2*(Q12+2*Q66)*n^2*m^2+Q22*m^4;
        Q66_bar(i)=(Q11+Q22-2*Q12-2*Q66)*m^2*n^2+Q66*(m^4+n^4);

        A11=A11+Q11_bar(i)*h;
        A12=A12+Q12_bar(i)*h;
```

```

        A22=A22+Q22_bar(i)*h;
    end

    A=[A11, A12; A12, A22]; %A matrix
    inv_a=inv(A);
    a11=inv_a(1,1);
    a12=inv_a(1,2);
    a22=inv_a(2,2);

    Vo=pi*R^2*L; % m^3

    Nx=F/(2*pi*R)+(P*R)/2; % sigmax*t
    Ny=P*R; % sigmay*t

    ex=a11*Nx+a12*Ny; % axial strain
    ey=a12*Nx+a22*Ny; % hoop strain

    Aend=pi*R^2;
    dVtube=(ex+2*ey)*Vo;
    Vf=Vo+dVtube;
    Lf=L+L*ex;
    Rf=(Vf/pi/Lf)^0.5;
    dR=Rf-R;
    Pclosed=-B*(ex+2*ey);

    Pintvec(jiter)=P;
    dVtubevec(jiter)=dVtube;
    err(jiter)=dR/R;
    Err(jiter)=P/(dR/R);

    Nxvec(jiter)=Nx;
    Nyvec(jiter)=Ny;

    Vfvec(jiter)=Vf;
    dxvec(jiter)=L*ex;
    dRvec(jiter)=dR;
end

thet=[0,10,20,30,40,50,60,70,80,90]
dll=[1.5E-3, -2.33E-2, -1.01E-1, -2.42E-1, -3.56E-1, -1.65E-1, 1.39E-1,
2.95E-1, 3.55E-1, 2.87E-1]; % values from Abaqus model

figure(2)
plot(thetavec,dxvec/L,'r')
xlabel('Wind Angle (degrees)','FontSize',24)
ylabel('Axial Strain (dL/L)','FontSize',24)
h=gca;
set(h,'FontSize',24,'LineWidth',2,'XTick',[0,10,20,30,40,50,60,70,80,90])
grid on
hold on
plot(thet,dll,'k--','LineWidth',2)
set(gcf,'Position',[0.0 0.0 900 600])
title('Tube Model Validation: Longitudinal Strain vs Wind Angle')
legend('Theoretical Solution','Tube Model with End Cap Force')

```

AB2: Codes used for multiple tube system parametric study

AB.2.1 MATLAB Code to create variable inputs for top loaded code in AB2.2

```
ANG=0:10:90; % degrees
PRESS=20:10:100; % psi
THICK=0.0011:0.0001:0.0018; % (m) inner radius values

for i=1:length(ANG);
    angl=ANG(i);
    for j=1:length(THICK);
        thick=THICK(j);
        thick2=thick;
        for k=1:length(PRESS);
            press=PRESS(k)*6894.757;
            jobn=['U3MultiT_a',num2str(angl),'_t',num2str(THICK(j)*10000),'_p',num2str(PRESS(k))];
            thick=num2str(thick);
            fid = fopen('Variables.py', 'w');
            fprintf(fid,'angl = %0.12f\n',angl);
            fprintf(fid,'press = %0.12f\n',press);
            fprintf(fid,'thick2=%0.12f\n',thick2);
            fprintf(fid,'thick = "%s"\n',thick);
            fprintf(fid,'jobn = "%s"\n',jobn);
            fclose(fid);

            %% run abq
            system('C:/Users/Melina/Desktop/Desktop/Research Grad/MacroforMulti');
            [flag]=system('abaqus cae noGUI=Change_DV_melinafreedisplacement.py');

        end
    end
end
```

AB2.2 Python code to create free displacement model and extract displacement results

```
import section
import regionToolset
import displayGroupMdbToolset as dgm
import part
import material
import assembly
import optimization
import step
import interaction
import load
import mesh
```

```

import job
import sketch
import visualization
import xyPlot
import displayGroupOdbToolset as dgo
import connectorBehavior

from part import *
from material import *
from section import *
from optimization import *
from assembly import *
from step import *
from interaction import *
from load import *
from mesh import *
from job import *
from sketch import *
from visualization import *
from connectorBehavior import *

session.journalOptions.setValues(replayGeometry=COORDINATE,
recoverGeometry=COORDINATE)

direc='C:/Users/Melina/Desktop/Desktop/Research Grad/MacroforMulti'
os.chdir(r"C:/Users/Melina/Desktop/Desktop/Research Grad/MacroforMulti")
#####
### LOAD VAR FILE #####
#####
execfile('Variables.py')

#####
### LOAD CAE FILE #####
#####

mdb.openAuxMdb(pathName=direc+'\BASEfreedispcNBC.cae')
mdb.copyAuxMdbModel(fromName='NewTrial', toName='NewTrial')
mdb.closeAuxMdb()

#####
### Fix radius partition 1 and 2 #####
#####

p = mdb.models['NewTrial'].parts['Solid']
s = p.features['Partition cell-1'].sketch
mdb.models['NewTrial'].ConstrainedSketch(name='__edit__', objectToCopy=s)

```

```

s1 = mdb.models['NewTrial'].sketches['__edit__']
g, v, d, c = s1.geometry, s1.vertices, s1.dimensions, s1.constraints
s1.setPrimaryObject(option=SUPERIMPOSE)
p.projectReferencesOntoSketch(sketch=s1,
    upToFeature=p.features['Partition cell-1'], filter=COPLANAR_EDGES)
s=mdb.models['NewTrial'].sketches['__edit__']
s.parameters['dimensions_0'].setValues(expression=thick)
s1.unsetPrimaryObject()
p = mdb.models['NewTrial'].parts['Solid']
p.features['Partition cell-1'].setValues(sketch=s1)
del mdb.models['NewTrial'].sketches['__edit__']
p = mdb.models['NewTrial'].parts['Solid']
p.regenerate()

## Fix radius partition 2 (Right tube)
p = mdb.models['NewTrial'].parts['Solid']
s = p.features['Partition cell-2'].sketch
mdb.models['NewTrial'].ConstrainedSketch(name='__edit__', objectToCopy=s)
s2 = mdb.models['NewTrial'].sketches['__edit__']
g, v, d, c = s2.geometry, s2.vertices, s2.dimensions, s2.constraints
s2.setPrimaryObject(option=SUPERIMPOSE)
p.projectReferencesOntoSketch(sketch=s2,
    upToFeature=p.features['Partition cell-2'], filter=COPLANAR_EDGES)
s=mdb.models['NewTrial'].sketches['__edit__']
s.parameters['dimensions_0'].setValues(expression=thick)
s2.unsetPrimaryObject()
p = mdb.models['NewTrial'].parts['Solid']
p.features['Partition cell-2'].setValues(sketch=s2)
del mdb.models['NewTrial'].sketches['__edit__']
p = mdb.models['NewTrial'].parts['Solid']
p.regenerate()

# #####
# ## Mesh Generation #####
# #####

p = mdb.models['NewTrial'].parts['Solid']
p.generateMesh()
a1 = mdb.models['NewTrial'].rootAssembly
a1.regenerate()
a = mdb.models['NewTrial'].rootAssembly

p1 = mdb.models['NewTrial'].parts['Solid']
session.viewports['Viewport: 1'].setValues(displayedObject=p1)
layupOrientation = None
p = mdb.models['NewTrial'].parts['Solid']
c = p.cells

```

```

cells = c.findAt(((0.003097, 0.000199, 0.0), ), ((0.003433, 0.000315, 0.0), ),
                ((-0.003163, -0.000211, 0.0), ), ((0.009631, 0.000335, 0.0), ), ((
                0.0096, -0.000414, 0.0), ), ((-0.003039, 0.000389, 0.0), ), ((0.003399,
                -0.000412, 0.0), ), ((0.003163, -0.00021, 0.0), ))
region1=regionToolset.Region(cells=cells)
p = mdb.models['NewTrial'].parts['Solid']
c = p.cells
cells = c.findAt(((0.003097, 0.000199, 0.0), ), ((0.003433, 0.000315, 0.0), ),
                ((-0.003163, -0.000211, 0.0), ), ((0.009631, 0.000335, 0.0), ), ((
                0.0096, -0.000414, 0.0), ), ((-0.003039, 0.000389, 0.0), ), ((0.003399,
                -0.000412, 0.0), ), ((0.003163, -0.00021, 0.0), ))
region2=regionToolset.Region(cells=cells)
compositeLayup = mdb.models['NewTrial'].parts['Solid'].compositeLayups['Solid']
compositeLayup.deletePlies()

#####
# ## Change Composite Angles #####
# #####
compositeLayup.CompositePly(suppressed=False, plyName='Ply-1', region=region1,
                             material='Carbonfiber', thicknessType=SPECIFY_THICKNESS, thickness=0.5,
                             orientationType=SPECIFY_ORIENT, orientationValue=angl,
                             additionalRotationType=ROTATION_NONE, additionalRotationField="",
                             axis=AXIS_3, angle=0.0, numIntPoints=1)
compositeLayup.CompositePly(suppressed=False, plyName='Ply-2', region=region2,
                             material='Carbonfiber', thicknessType=SPECIFY_THICKNESS, thickness=0.5,
                             orientationType=SPECIFY_ORIENT, orientationValue=-angl,
                             additionalRotationType=ROTATION_NONE, additionalRotationField="",
                             axis=AXIS_3, angle=0.0, numIntPoints=1)
a = mdb.models['NewTrial'].rootAssembly
a.regenerate()
session.viewports['Viewport: 1'].setValues(displayedObject=a)
session.viewports['Viewport: 1'].assemblyDisplay.setValues(loads=ON, bcs=ON,
                                                           predefinedFields=ON, connectors=ON)

# #####
# ## Change Internal Pressurization #####
# #####
mdb.models['NewTrial'].loads['pressure'].setValues(magnitude=press)
session.viewports['Viewport: 1'].assemblyDisplay.setValues(loads=OFF, bcs=OFF,
                                                           predefinedFields=OFF, connectors=OFF)

##### Fixing nodeset #####
p = mdb.models['NewTrial'].parts['Solid']
n = p.nodes
nodes = n[80:87]+n[93:97]+n[98:99]+n[3451:3456]+n[3589:3714]+n[3842:3844]+\
        n[3851:3853]+n[4155:4159]+n[4175:4180]+n[4204:4326]+n[4328:4331]

```

```

p.Set(nodes=nodes, name='nodesTop')
session.viewports['Viewport: 1'].partDisplay.setValues(mesh=OFF)
a = mdb.models['NewTrial'].rootAssembly
a.regenerate()
session.viewports['Viewport: 1'].setValues(displayedObject=a)
session.viewports['Viewport: 1'].assemblyDisplay.setValues(loads=OFF, bcs=OFF,
    predefinedFields=OFF, connectors=OFF, optimizationTasks=OFF,
    geometricRestrictions=OFF, stopConditions=OFF)

#### Fix single center node#####
session.viewports['Viewport: 1'].partDisplay.setValues(mesh=ON)
p = mdb.models['NewTrial'].parts['Solid']
n = p.nodes
nodes = n[13732:13735]+n[13792:13794]
p.Set(nodes=nodes, name='cent')
session.viewports['Viewport: 1'].partDisplay.setValues(mesh=OFF)
a = mdb.models['NewTrial'].rootAssembly
a.regenerate()
session.viewports['Viewport: 1'].setValues(displayedObject=a)
session.viewports['Viewport: 1'].assemblyDisplay.setValues(
    optimizationTasks=OFF, geometricRestrictions=OFF, stopConditions=OFF)

#####Fix Midline#####
p = mdb.models['NewTrial'].parts['Solid']
n = p.nodes
nodes = n[83:84]+n[85:87]+n[3711:3714]+n[3842:3844]+n[3851:3853]+n[4328:4331]
p.Set(nodes=nodes, name='midline')

# #####
# ## Run (or not) Singe_iter.py #####
# #####
## Jobname
mdb.saveAs('RUN.cae')

mdb.Job(name=jobn, model='NewTrial', description="",
    type=ANALYSIS, atTime=None, waitMinutes=0, waitHours=0, queue=None,
    memory=90, memoryUnits=PERCENTAGE, getMemoryFromAnalysis=True,
    explicitPrecision=SINGLE, nodalOutputPrecision=SINGLE, echoPrint=OFF,
    modelPrint=OFF, contactPrint=OFF, historyPrint=OFF, userSubroutine="",
    scratch="", multiprocessingMode=DEFAULT, numCpus=1, numGPUs=0)

mdb.jobs[jobn].submit(consistencyChecking=OFF)
mdb.jobs[jobn].waitForCompletion()

```

```

#####
#-Collecting Outputs-----
# #####
filename=dir+'+jobn+'.odb'
odb = openOdb(path=filename)
top_region=odb.rootAssembly.instances['SOLID-1'].nodeSets['MIDLINE']

disp=odb.steps['load'].frames[-1].fieldOutputs['U']
regdisp=disp.getSubset(region=top_region).values
import numpy
mylist=[]
for v in regdisp:
    k=v.data[1]
    mylist.append(k)

U2av=numpy.mean(mylist)
U2mx=max(mylist)
U2mn=min(mylist)
press=press/6894.757

# print 'Angle= %10.4f, Pressure= %10.4f, LatexThickness= %10.4E, Max U2 at top= %10.4E
\n'% (angl,press,thick2,U2mx)
outputFile = open(dir+'RESULTSfreedispNBC.dat','a')
outputFile.write('%10.4f %10.4f %10.4E %10.4E %10.4E %10.4E \n' %
(angl,press,thick2,U2av,U2mx,U2mn))

outputFile.close()
odb.close()

#####
#-COMPLETE-----
#####

```

AB.2.3 MATLAB Code to create variable inputs for top loaded code in AB2.4

```
ANG=0:10:90; %degrees
PRESS=10:10:100; %psi
THICK=0.0014:0.0001:0.0020; %m inner radius values
TOP=[50000,100000,400000]; %Pa
Emodulus[,1030000,10300000]; %Pa
CF=[0.003]; %m

for i=1:length(ANG);
    angl=ANG(i);
    for j=1:length(THICK);
        thick=THICK(j);
        thick2=thick;
        for k=1:length(PRESS);
            press=PRESS(k)*6894.757;
            for m=1:length(TOP);
                top=TOP(m);
                for n=1:length(Emodulus);
                    E=Emodulus(n);
                    for p=1:length(CF);
                        cf=CF(p);
                        cf2=cf;

jobn=['stressMultiT_a',num2str(angl),'_t',num2str(THICK(j)*10000),'_p',num2str(PRESS(k)),'_ts',num2str(TOP(m))
,'_E',num2str(Emodulus(n)),'_cf',num2str(CF(p)*10000)];
                thick=num2str(thick);
                cf=num2str(cf);
                fid = fopen('Variables.py', 'w');
                fprintf(fid,'angl = %0.12f\n',angl);
                fprintf(fid,'press = %0.12f\n',press);
                fprintf(fid,'thick2=%0.12f\n',thick2);
                fprintf(fid,'thick = "%s"\n',thick);
                fprintf(fid,'jobn = "%s"\n',jobn);
                fprintf(fid,'top = %0.12f\n',top);
                fprintf(fid,'E = %0.12f\n',E);
                fprintf(fid,'cf2=%0.12f\n',cf2);
                fprintf(fid,'cf="%s"\n',cf);
                fclose(fid);

                %% run abq
                system('C:/Users/Melina/Desktop/Desktop/Research Grad/MacroforMulti');
                [flag]=system('abaqus cae noGUI=Change_DV_melinatopforce.py');

            end
        end
    end
end
end
end
```

AB2.4 Python code to create top loaded model and extract displacement results

```
import section
import regionToolset
import displayGroupMdbToolset as dgm
import part
import material
import assembly
import optimization
import step
import interaction
import load
import mesh
import job
import sketch
import visualization
import xyPlot
import displayGroupOdbToolset as dgo
import connectorBehavior

from part import *
from material import *
from section import *
from optimization import *
from assembly import *
from step import *
from interaction import *
from load import *
from mesh import *
from job import *
from sketch import *
from visualization import *
from connectorBehavior import *

session.journalOptions.setValues(replayGeometry=COORDINATE,
recoverGeometry=COORDINATE)

direc='C:/Users/Melina/Desktop/Desktop/Research Grad/MacroforMulti'
os.chdir(r"C:/Users/Melina/Desktop/Desktop/Research Grad/MacroforMulti")
#####
### LOAD VAR FILE #####
#####
execfile('Variables.py')

#####
### LOAD CAE FILE #####
#####
```

```

mdb.openAuxMdb(pathName=dir+'\\BASEtopforceNBC.cae')
mdb.copyAuxMdbModel(fromName='NewTrial', toName='NewTrial')
mdb.closeAuxMdb()

```

```

#####
# ## Fix radius partition 1 and 2 #####
#####

```

```

p = mdb.models['NewTrial'].parts['Solid']
s = p.features['Partition cell-1'].sketch
mdb.models['NewTrial'].ConstrainedSketch(name='__edit__', objectToCopy=s)
s1 = mdb.models['NewTrial'].sketches['__edit__']
g, v, d, c = s1.geometry, s1.vertices, s1.dimensions, s1.constraints
s1.setPrimaryObject(option=SUPERIMPOSE)
p.projectReferencesOntoSketch(sketch=s1,
    upToFeature=p.features['Partition cell-1'], filter=COPLANAR_EDGES)
s=mdb.models['NewTrial'].sketches['__edit__']
s.parameters['dimensions_0'].setValues(expression=thick)
s1.unsetPrimaryObject()
p = mdb.models['NewTrial'].parts['Solid']
p.features['Partition cell-1'].setValues(sketch=s1)
del mdb.models['NewTrial'].sketches['__edit__']
p = mdb.models['NewTrial'].parts['Solid']
p.regenerate()

```

```

## Fix radius partition 2 (Right tube)
p = mdb.models['NewTrial'].parts['Solid']
s = p.features['Partition cell-2'].sketch
mdb.models['NewTrial'].ConstrainedSketch(name='__edit__', objectToCopy=s)
s2 = mdb.models['NewTrial'].sketches['__edit__']
g, v, d, c = s2.geometry, s2.vertices, s2.dimensions, s2.constraints
s2.setPrimaryObject(option=SUPERIMPOSE)
p.projectReferencesOntoSketch(sketch=s2,
    upToFeature=p.features['Partition cell-2'], filter=COPLANAR_EDGES)
s=mdb.models['NewTrial'].sketches['__edit__']
s.parameters['dimensions_0'].setValues(expression=thick)
s2.unsetPrimaryObject()
p = mdb.models['NewTrial'].parts['Solid']
p.features['Partition cell-2'].setValues(sketch=s2)
del mdb.models['NewTrial'].sketches['__edit__']
p = mdb.models['NewTrial'].parts['Solid']
p.regenerate()

```

```

#####
##### Setting Carbon Fiber Thickness #####

```

```
#####
```

```
p = mdb.models['NewTrial'].parts['Solid']
s = p.features['Partition cell-1'].sketch
mdb.models['NewTrial'].ConstrainedSketch(name='__edit__', objectToCopy=s)
s2 = mdb.models['NewTrial'].sketches['__edit__']
g, v, d, c = s2.geometry, s2.vertices, s2.dimensions, s2.constraints
s2.setPrimaryObject(option=SUPERIMPOSE)
p.projectReferencesOntoSketch(sketch=s2,
    upToFeature=p.features['Partition cell-1'], filter=COPLANAR_EDGES)
s=mdb.models['NewTrial'].sketches['__edit__']
s.parameters['cf_ri'].setValues(expression=cf)
s2.unsetPrimaryObject()
p = mdb.models['NewTrial'].parts['Solid']
p.features['Partition cell-1'].setValues(sketch=s2)
del mdb.models['NewTrial'].sketches['__edit__']
p = mdb.models['NewTrial'].parts['Solid']
```

```
s = p.features['Partition cell-2'].sketch
mdb.models['NewTrial'].ConstrainedSketch(name='__edit__', objectToCopy=s)
s1 = mdb.models['NewTrial'].sketches['__edit__']
g, v, d, c = s1.geometry, s1.vertices, s1.dimensions, s1.constraints
s1.setPrimaryObject(option=SUPERIMPOSE)
p.projectReferencesOntoSketch(sketch=s1,
    upToFeature=p.features['Partition cell-2'], filter=COPLANAR_EDGES)
s=mdb.models['NewTrial'].sketches['__edit__']
s.parameters['cf_ri'].setValues(expression=cf)
s1.unsetPrimaryObject()
p = mdb.models['NewTrial'].parts['Solid']
p.features['Partition cell-2'].setValues(sketch=s1)
del mdb.models['NewTrial'].sketches['__edit__']
p = mdb.models['NewTrial'].parts['Solid']
p.regenerate()
a = mdb.models['NewTrial'].rootAssembly
a.regenerate()
session.viewports['Viewport: 1'].setValues(displayedObject=a)
session.viewports['Viewport: 1'].assemblyDisplay.setValues(mesh=ON,
    optimizationTasks=OFF, geometricRestrictions=OFF, stopConditions=OFF)
session.viewports['Viewport: 1'].assemblyDisplay.meshOptions.setValues(
    meshTechnique=ON)
```

```
# #####
# ## Mesh Generation #####
# #####
```

```
p = mdb.models['NewTrial'].parts['Solid']
p.generateMesh()
```

```

a1 = mdb.models['NewTrial'].rootAssembly
a1.regenerate()
a = mdb.models['NewTrial'].rootAssembly

p1 = mdb.models['NewTrial'].parts['Solid']
session.viewports['Viewport: 1'].setValues(displayedObject=p1)
layupOrientation = None
p = mdb.models['NewTrial'].parts['Solid']
c = p.cells
cells = c.findAt(((0.003097, 0.000199, 0.0), ), ((0.003433, 0.000315, 0.0), ),
                ((-0.003163, -0.000211, 0.0), ), ((0.009631, 0.000335, 0.0), ), ((
                0.0096, -0.000414, 0.0), ), ((-0.003039, 0.000389, 0.0), ), ((0.003399,
                -0.000412, 0.0), ), ((0.003163, -0.00021, 0.0), ))
region1=regionToolset.Region(cells=cells)
p = mdb.models['NewTrial'].parts['Solid']
c = p.cells
cells = c.findAt(((0.003097, 0.000199, 0.0), ), ((0.003433, 0.000315, 0.0), ),
                ((-0.003163, -0.000211, 0.0), ), ((0.009631, 0.000335, 0.0), ), ((
                0.0096, -0.000414, 0.0), ), ((-0.003039, 0.000389, 0.0), ), ((0.003399,
                -0.000412, 0.0), ), ((0.003163, -0.00021, 0.0), ))
region2=regionToolset.Region(cells=cells)
compositeLayup = mdb.models['NewTrial'].parts['Solid'].compositeLayups['Solid']
compositeLayup.deletePlies()

# #####
# ## Change Composite Angles #####
# #####
compositeLayup.CompositePly(suppressed=False, plyName='Ply-1', region=region1,
    material='Carbonfiber', thicknessType=SPECIFY_THICKNESS, thickness=0.5,
    orientationType=SPECIFY_ORIENT, orientationValue=angl,
    additionalRotationType=ROTATION_NONE, additionalRotationField=",
    axis=AXIS_3, angle=0.0, numIntPoints=1)
compositeLayup.CompositePly(suppressed=False, plyName='Ply-2', region=region2,
    material='Carbonfiber', thicknessType=SPECIFY_THICKNESS, thickness=0.5,
    orientationType=SPECIFY_ORIENT, orientationValue=-angl,
    additionalRotationType=ROTATION_NONE, additionalRotationField=",
    axis=AXIS_3, angle=0.0, numIntPoints=1)
a = mdb.models['NewTrial'].rootAssembly
a.regenerate()
session.viewports['Viewport: 1'].setValues(displayedObject=a)
session.viewports['Viewport: 1'].assemblyDisplay.setValues(loads=ON, bcs=ON,
    predefinedFields=ON, connectors=ON)

# #####
# ## Change Internal Pressurization #####
# #####

```

```
mdb.models['NewTrial'].loads['pressure'].setValues(magnitude=press)
session.viewports['Viewport: 1'].assemblyDisplay.setValues(loads=OFF, bcs=OFF,
    predefinedFields=OFF, connectors=OFF)
```

```
#####
##### Fixing nodeset #####
#####
```

```
p = mdb.models['NewTrial'].parts['Solid']
n = p.nodes
nodes = n[80:87]+n[93:97]+n[98:99]+n[3451:3456]+n[3589:3714]+n[3842:3844]+\
    n[3851:3853]+n[4155:4159]+n[4175:4180]+n[4204:4326]+n[4328:4331]
p.Set(nodes=nodes, name='nodesTop')
session.viewports['Viewport: 1'].partDisplay.setValues(mesh=OFF)
a = mdb.models['NewTrial'].rootAssembly
a.regenerate()
session.viewports['Viewport: 1'].setValues(displayedObject=a)
session.viewports['Viewport: 1'].assemblyDisplay.setValues(loads=OFF, bcs=OFF,
    predefinedFields=OFF, connectors=OFF, optimizationTasks=OFF,
    geometricRestrictions=OFF, stopConditions=OFF)
```

```
#####
#### Fix single center node #####
#####
```

```
p1 = mdb.models['NewTrial'].parts['Solid']
p = mdb.models['NewTrial'].parts['Solid']
n = p.nodes
nodes = n[3508:3510]+n[3761:3763]+n[12368:12370]+n[12490:12492]+n[13460:13462]+\
    n[13522:13524]+n[13584:13586]+n[13889:13893]+n[19073:19075]+\
    n[19195:19197]
p.Set(nodes=nodes, name='cent')
```

```
#####
##### Fix Single Center Node #####
#####
```

```
p = mdb.models['NewTrial'].parts['Solid']
n = p.nodes
nodes = n[13801:13802]
p.Set(nodes=nodes, name='one')
```

```
#####
##### Fix Midline #####
#####
```

```
p = mdb.models['NewTrial'].parts['Solid']
n = p.nodes
```

```
nodes = n[83:84]+n[85:87]+n[3711:3714]+n[3842:3844]+n[3851:3853]+n[4328:4331]
p.Set(nodes=nodes, name='midline')
```

```
#####
##### Change E #####
#####
mdb.models['NewTrial'].materials['Vytaflex 20'].elastic.setValues(table=((
    E, 0.499), ))
```

```
#####
#####Change top load #####
#####
```

```
mdb.models['NewTrial'].loads['topload'].setValues(magnitude=top)
#####
# ## Run (or not) Singe_iter.py #####
#####
## Jobname
mdb.saveAs('RUN.cae')
```

```
mdb.Job(name=jobn, model='NewTrial', description="",
        type=ANALYSIS, atTime=None, waitMinutes=0, waitHours=0, queue=None,
        memory=90, memoryUnits=PERCENTAGE, getMemoryFromAnalysis=True,
        explicitPrecision=SINGLE, nodalOutputPrecision=SINGLE, echoPrint=OFF,
        modelPrint=OFF, contactPrint=OFF, historyPrint=OFF, userSubroutine="",
        scratch="", multiprocessingMode=DEFAULT, numCpus=1, numGPUs=0)
```

```
mdb.jobs[jobn].submit(consistencyChecking=OFF)
mdb.jobs[jobn].waitForCompletion()
#####
#-Collecting Outputs-----
#####
filename=dir+'+jobn+'.odb'
odb = openOdb(path=filename)
top_region=odb.rootAssembly.instances['SOLID-1'].nodeSets['MIDLINE']
```

```
disp=odb.steps['load'].frames[-1].fieldOutputs['U']
regdisp=disp.getSubset(region=top_region).values
mylist=[]
```

```
import numpy
for v in regdisp:
    k=v.data[1]
    mylist.append(k)
```

```
U2av=numpy.mean(mylist)
```

```
U2mn=min(mylist)
U2mx=max(mylist)
press=press/6894.757
```

```
outputFile = open(direc+'/RESULTStopforce.dat','a')
outputFile.write('%10.4f %10.4f %10.4E %10.4E %10.4E %10.4E %10.4E
%10.4E %10.4E\n' % (angl,press,thick2,top,E,cf2,U2av,U2mn,U2mx))
```

```
outputFile.close()
odb.close()
```

```
#-----
#-COMPLETE-----
#-----
```